Mitochondrial respiratory states and rates: Building blocks of mitochondrial physiology

Part 1. MitoEAGLE preprint 2018-03-03(33)

http://www.mitoeagle.org/index.php/MitoEAGLE_preprint_2018-02-08
Preprint version 33 (2018-03-03)

MitoEAGLE Network

Corresponding author: Gnaiger E

Co-authors:

Aasander Frostner E, Acuna-Castroviejo D, Ahn B, Alves MG, Amati F, Aral C, Arandarčikaitė O, Bailey DM, Bakker BM, Bastos Sant'Anna Silva AC, Battino M, Beard DA, Ben-Shachar D, Bishop D, Borsheim E, Borutaitė V, Bouillaud F, Breton S, Brown GC, Brown RA, Buettner GR, Burtscher J, Calabria E, Calbet JA, Calzia E, Cardoso LHD, Carvalho E, Casado Pinna M, Cervinkova Z, Chang SC, Chaurasia B, Chen Q, Chicco AJ, Chinopoulos C, Clementi E, Coen PM, Collin A, Crisóstomo L, Das AM, Davis MS, De Palma C, Dias TR, Distefano G, Doerrier C, Drahota Z, Duchen MR, Durham WJ, Ehinger J, Elmer E, Endlicher R, Fell DA, Ferko M, Ferreira JCB, Ferreira R, Filipovska A, Fisar Z, Fischer M, Fisher JJ, Fornaro M, Galkin A, Garcia-Roves PM, Garcia-Souza LF, Garten A, Genova ML, Giovarelli M, Gonzalez-Armenta JL, Gonzalo H, Goodpaster BH, Gorr TA, Gourlay CW, Granata C, Grefte S, Haas CB, Haavik J, Han J, Harrison DK, Hellgren KT, Hernansanz-Agustin P, Holland OJ, Hoppel CL, Houstek J, Hunger M, Iglesias-Gonzalez J, Irving BA, Iyer S, Jackson CB, Jadiya P, Jang DH, Jansen-Dürr P, Jespersen NR, Jha RK, Jurk D, Kaambre T, Kane DA, Kappler L, Karabatsiakis A, Keijer J, Keppner G, Khamoui AV, Klingenspor M, Komlodi T, Koopman WJH, Kopitar-Jerala N, Krajcova A, Krako Jakovljevic N, Kuang J, Kucera O, Labieniec-Watala M, Lai N, Laner V, Larsen TS, Lee HK, Leeuwenburgh C, Lemieux H, Lerfall J, Liu J, Lucchinetti E, Macedo MP, MacMillan-Crow LA, Makrecka-Kuka M, Malik A, Markova M, Meszaros AT, Michalak S, Moisoi N, Molina AJA, Montaigne D, Moore AL, Moreira BP, Mracek T, Muntane J, Muntean DM, Murray AJ, Nemec M, Neuzil J, Newsom S, Nozickova K, O'Gorman D, Oliveira MT, Oliveira PF, Oliveira PJ, Orynbayeva Z, Pak YK, Palmeira CM, Passos JF, Patel HH, Pecina P, Pelnena D, Pereira da Silva Grilo da Silva F, Pesta D, Petit PX, Pichaud N, Piel S, Pirkmajer S, Porter RK, Pranger F, Prochownik EV, Pulinilkunnil T, Puurand M, Radenkovic F, Radi R, Ramzan R, Reboredo P, Renner-Sattler K, Robinson MM, Rohlena J, Rolo AP, Ropelle ER, Røsland GV, Rossiter HB, Rybacka-Mossakowska J, Saada A, Safaei Z, Salvadego D, Sandi C, Scatena R, Schartner M, Scheibye-Knudsen M, Schilling JM, Schlattner U, Schönfeld P, Schwarzer C, Scott GR, Shabalina IG, Sharma P, Sharma V, Shevchuk I, Siewiera K, Silber AM, Silva AM, Singer D, Smenes BT, Soares FAA, Sobotka O, Sokolova I, Spinazzi M, Stankova P, Stier A, Stocker R, Sumbalova Z, Suravajhala P, Swerdlow RH, Swiniuch D, Tanaka M, Tandler B, Tavernarakis N, Tepp K, Thyfault JP, Tomar D, Towheed A, Tretter L, Trifunovic A, Trivigno C, Tronstad KJ, Trougakos IP, Tyrrell DJ, Urban T, Valentine JM, Velika B, Vendelin M, Vercesi AE, Victor VM, Villena JA, Vitorino RMP, Vogt S, Volani C, Votion DM, Vujacic-Mirski K, Wagner BA, Ward ML, Watala C, Wei YH, Wieckowski MR, Williams C, Wohlwend M, Wolff J, Wüst RCI, Zaugg K, Zaugg M, Zischka H, Zorzano A

Supporting:

Bernardi P, Boetker HE, Bouitbir J, Coker RH, Dubouchaud H, Dyrstad SE, Engin AB, Gan Z, Garlid KD, Haendeler J, Hand SC, Hepple RT, Hickey AJ, Hoel F, Kainulainen H, Kowaltowski AJ, Lane N, Lenaz G, Liu SS, Mazat JP, Menze MA, Methner A, Nedergaard J, Pallotta ML, Parajuli N, Pettersen IKN, Porter C, Salin K, Sazanov LA, Skolik R, Sonkar VK, Szabo I, Vieyra A

Updates and discussion:
http://www.mitoeagle.org/index.php/MitoEAGLE_preprint_2018-02-08

Correspondence: Gnaiger E
Chair COST Action CA15203 MitoEAGLE – http://www.mitoeagle.org
Department of Visceral, Transplant and Thoracic Surgery, D. Swarovski Research Laboratory, Medical University of Innsbruck, Innrain 66/4, A-6020 Innsbruck, Austria
Email: mitoeagle@i-med.ac.at
Tel: +43 512 566796, Fax: +43 512 566796 20

Contents

Abstract As the knowledge base and importance of mitochondrial physiology to human health expands, the necessity for harmonizing nomenclature concerning mitochondrial respiratory states and rates has become increasingly apparent. Clarity of concept and consistency of nomenclature are key trademarks of a research field. These features facilitate effective transdisciplinary communication, education, and ultimately further discovery. The chemiosmotic theory establishes the mechanism of energy transformation and coupling in oxidative phosphorylation. The unifying concept of the protonmotive force provides the framework for developing a consistent theoretical foundation of mitochondrial physiology and bioenergetics. We follow IUPAC guidelines on terminology in physical chemistry, extended by considerations on open systems and irreversible thermodynamics. The concept-driven constructive terminology incorporates the meaning of each quantity and aligns concepts and symbols to the nomenclature of classical bioenergetics. In the frame of COST Action MitoEAGLE open to global bottom-up input, we endeavour to provide a balanced view on mitochondrial respiratory control and a critical discussion on reporting data of mitochondrial respiration in terms of metabolic flows and fluxes. Uniform standards for evaluation of respiratory states and rates will ultimately support the development of databases of mitochondrial respiratory function in species, tissues, and cells.

Keywords: Mitochondrial respiratory control, coupling control, mitochondrial preparations, protonmotive force, uncoupling, oxidative phosphorylation, OXPHOS, efficiency, electron transfer, ET; proton leak, LEAK, residual oxygen consumption, ROX, State 2, State 3, State 4, normalization, flow, flux, O_2

Executive summary

1. In view of the broad implications for health care, mitochondrial researchers face an increasing responsibility to disseminate their fundamental knowledge and novel discoveries to a wide range of stakeholders and scientists beyond the group of specialists. This requires implementation of a commonly accepted terminology within the discipline and standardization in the translational context. Authors, reviewers, journal editors, and lecturers are challenged to collaborate with the aim to harmonize the nomenclature in the growing field of mitochondrial physiology and bioenergetics.
2. Aerobic respiration depends on the coupling of phosphorylation (ADP → ATP) to O_2 flux in catabolic reactions. Coupling in oxidative phosphorylation is mediated by translocation of protons across the inner mitochondrial membrane through proton pumps generating or utilizing the protonmotive force, measured between the mitochondrial matrix and intermembrane compartment. Compartmental coupling distinguishes vectorial oxidative phosphorylation from glycolytic fermentation as the counterpart of cellular core energy metabolism (**Figure 1**).
3. To exclude fermentation and other cytosolic interactions from exerting an effect on the analysis of mitochondrial metabolism, the barrier function of the plasma membrane must be disrupted. Selective removal or permeabilization of the plasma membrane yields mitochondrial preparations—including isolated mitochondria, tissue and cellular preparations—with structural and functional integrity. Then extra-mitochondrial concentrations of fuel substrates, ADP, ATP, inorganic phosphate, and cations including H^+ can be controlled to determine mitochondrial function under a set of conditions defined as coupling control states. A concept-driven terminology of bioenergetics explicitly incorporates in its terms and symbols information on the nature of respiratory states that makes the technical terms readily recognized and more easy to understand.

Figure 1. Mitochondrial respiration with reduction of O_2 catalysed by the electron transfer system, ETS (*a*), catabolic respiration (including non-mitochondrial oxidation reactions, *b*), and oxygen balance of internal (*c*) and external (*d*) respiration

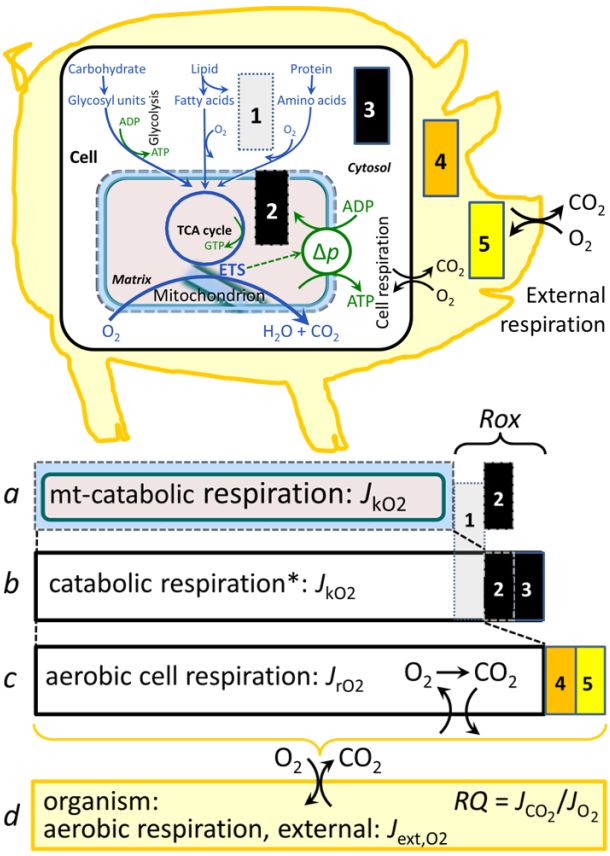

All chemical reactions, r, that consume O_2 in the cells of an organism, contribute to cell respiration, J_{rO_2}. ❶ Non-mitochondrial O_2 consumption by catabolic reactions, particularly peroxisomal oxidases; ❷ mitochondrial residual oxygen consumption, *Rox*, after blocking the ETS; ❸ non-mitochondrial *Rox*; ❹ extracellular O_2 consumption; ❺ aerobic microbial respiration. Bars are not at a quantitative scale.

a **Mitochondrial catabolic respiration**, J_{kO_2}, is the O_2 consumption by the mitochondrial ETS maintaining the protonmotive force, Δp. J_{kO_2} excludes *Rox*.

b **Catabolic respiration** is the O_2 consumption associated with catabolic pathways in the cell, including peroxisomal oxidation reactions (❶) in addition to mitochondrial catabolism (* The reactions k have to be defined specifically for *a* and *b*.)

c **Aerobic cell respiration**, J_{rO_2}, takes into account internal O_2-consuming reactions, r, including catabolic respiration and *Rox*. Internal respiration of an organism includes extracellular O_2 consumption (❹) and aerobic respiration by the microbiome (❺). Respiration is distinguished from fermentation by: (*1*) External electron acceptors for the maintenance of redox balance, whereas fermentation is characterized by an internal electron acceptor produced in intermediary metabolism. In aerobic cell respiration, redox balance is maintained by O_2 as the electron acceptor. (*2*) Compartmental coupling in vectorial oxidative phosphorylation, in contrast to exclusively scalar substrate-level phosphorylation in fermentation.

d **External respiration** balances internal respiration at steady-state. O_2 is transported from the environment across the respiratory cascade (circulation between tissues and diffusion across cell membranes) to the intracellular compartment, while bicarbonate and CO_2 are transported in reverse to the extracellular mileu and the organismic environment. Hemoglobin provides the molecular paradigm for the combination of O_2 and CO_2 exchange, as do lungs and gills on the morphological level. The respiratory quotient, *RQ*, is the molar CO_2/O_2 exchange ratio; when combined with the respiratory nitrogen quotient, N/O_2 (mol N given off per mol O_2 consumed), the *RQ* reflects the proportion of carbohydrate, lipd and protein utilized in cell respiration during aerobically balanced steady-states.

4. Mitochondrial coupling states are defined according to the control of respiratory oxygen flux by the protonmotive force. Capacities of oxidative phosphorylation and electron transfer are measured at kinetically saturating concentrations of fuel substrates, ADP and inorganic phosphate, or at optimal uncoupler concentrations, respectively. Respiratory capacity is a measure of the upper bound of the rate of respiration, depends on the substrate type undergoing oxidation, and provides reference values for the diagnosis of health and disease, and for evaluation of the

effects of **E**volutionary background, **A**ge, **G**ender and sex, **L**ifestyle and **E**nvironment (EAGLE).

5. Incomplete tightness of coupling, *i.e.*, some degree of uncoupling relative to the substrate-dependent coupling stoichiometry, is a characteristic of energy-transformations across membranes. Uncoupling is caused by a variety of physiological, pathological, toxicological, pharmacological and environmental conditions that exert an influence not only on the proton leak and cation cycling, but also on proton slip within the proton pumps and the structural integrity of the mitochondria. A more loosely coupled state is induced by stimulation of mitochondrial superoxide formation and the bypass of proton pumps. In addition, uncoupling by application of protonophores represents an experimental intervention for the transition from a well-coupled to the noncoupled state of mitochondrial respiration.
6. Respiratory oxygen consumption rates have to be carefully normalized to enable meta-analytic studies beyond the specific question of a particular experiment. Therefore, all raw data should be published in a supplemental table or open access data repository. Normalization of rates for the volume of the experimental chamber (the measuring system) is distinguished from normalization for: (*1*) the volume or mass of the experimental sample; (*2*) the number of objects (cells, organisms); and (*3*) the concentration of mitochondrial markers in the chamber.
7. The consistent use of terms and symbols will facilitate transdisciplinary communication and support further developments of a database on bioenergetics and mitochondrial physiology. The present considerations are focused on studies with mitochondrial preparations. These will be extended in a series of reports on pathway control of mitochondrial respiration, the protonmotive force, respiratory states in intact cells, and harmonization of experimental procedures.

Box 1: In brief – Mitochondria and Bioblasts

'*For the physiologist, mitochondria afforded the first opportunity for an experimental approach to structure-function relationships, in particular those involved in active transport, vectorial metabolism, and metabolic control mechanisms on a subcellular level*' (Ernster and Schatz 1981).

Mitochondria are the oxygen-consuming electrochemical generators evolved from endosymbiotic bacteria (Margulis 1970; Lane 2005). They were described by Richard Altmann (1894) as 'bioblasts', which include not only the mitochondria as presently defined, but also symbiotic and free-living bacteria. The word 'mitochondria' (Greek mitos: thread; chondros: granule) was introduced by Carl Benda (1898).

Mitochondria are dynamic networks contained within eukaryotic cells morphologically characterized by a double membrane. The mitochondrial inner membrane (mtIM) shows dynamic tubular to disk-shaped cristae that separate the mitochondrial matrix, *i.e.*, the negatively charged internal mitochondrial compartment, from the intermembrane space; the latter being positively charged and enclosed by the mitochondrial outer membrane (mtOM). The mtIM contains the non-bilayer phospholipid cardiolipin, which is not present in any other eukaryotic cellular membrane. Cardiolipin promotes the formation of respiratory supercomplexes (SC $I_nIII_nIV_n$), which are supramolecular assemblies based upon specific, though dynamic interactions between individual respiratory complexes (Greggio *et al.* 2017; Lenaz *et al.* 2017). Membrane fluidity exerts an influence on functional properties of proteins incorporated in the membranes (Waczulikova *et al.* 2007). In addition to mitochondrial movement along microtubules, mitochondrial morphology can change in response to energy

requirements of the cell via processes known as fusion and fission, through which mitochondria communicate within a network, and in response to intracellular stress factors causing swelling and ultimately permeability transition.

Mitochondria are the structural and functional elements of cell respiration. Mitochondrial respiration is the reduction of oxygen by electron transfer coupled to electrochemical proton translocation across the mtIM. In the process of oxidative phosphorylation (OXPHOS), the catabolic reaction of oxygen consumption is electrochemically coupled to the transformation of energy in the form of adenosine triphosphate (ATP; Mitchell 1961, 2011). Mitochondria are the powerhouses of the cell which contain the machinery of the OXPHOS-pathways, including transmembrane respiratory complexes (proton pumps with FMN, Fe-S and cytochrome *b*, *c*, aa_3 redox systems); alternative dehydrogenases and oxidases; the coenzyme ubiquinone (Q); F-ATPase or ATP synthase; the enzymes of the tricarboxylic acid cycle, fatty acid and aminoacid oxidation; transporters of ions, metabolites and co-factors; and mitochondrial kinases related to energy transfer pathways. The mitochondrial proteome comprises over 1,200 proteins (Calvo *et al.* 2015; 2017), mostly encoded by nuclear DNA (nDNA), with a variety of functions, many of which are relatively well known (*e.g.*, proteins regulating mitochondrial biogenesis or apoptosis), while others are still under investigation, or need to be identified (*e.g.*, alanine transporter). Only lately it is possible to use the mammalian mitochondrial proteome to discover and characterize the genetic basis of mitochondrial diseases (Williams *et al.* 2016; Palmfeldt and Bross 2017).

There is a constant crosstalk between mitochondria and the other cellular components. The crosstalk between mitochondria and endoplasmic reticulum is involved in the regulation of calcium homeostasis, cell division, autophagy, differentiation, and anti-viral signaling (Murley and Nunnari 2016). Mitochondria contribute to the formation of peroxisomes, which are hybrids of mitochondrial and ER-derived precursors (Sugiura *et al.* 2017). Cellular mitochondrial homeostasis (mitostasis) is maintained through regulation at both the transcriptional and post-translational level. Cell signalling modules contribute to homeostatic regulation throughout the cell cycle or even cell death by activating proteostatic modules (*e.g.*, the ubiquitin-proteasome and autophagy-lysosome pathways) and genome stability modules in response to varying energy demands and stress cues (Quiros *et al.* 2016). Mitochondria can traverse cell boundaries in a process known as horizontal mitochondrial transfer between cells (Torralba *et al.* 2016).

Mitochondria typically maintain several copies of their own circular genome known as mitochondrial DNA (mtDNA; hundred to thousands per cell; Cummins 1998), which is maternally inherited. Biparental mitochondrial inheritance is documented in mammals, birds, fish, reptiles and invertebrate groups, and is even the norm in bivalves (Breton *et al.* 2007; White *et al.* 2008). mtDNA is compact (16.5 kB in humans) and encodes 13 protein subunits of the transmembrane respiratory Complexes CI, CIII, CIV and F-ATPase, 22 tRNAs, and two RNAs. Additional gene content has been suggested to include microRNAs, piRNA, smithRNAs, repeat associated RNA, and even additional proteins (Duarte *et al.* 2014; Lee *et al.* 2015; Cobb *et al.* 2016). The mitochondrial genome requires nuclear-encoded mitochondrially targeted proteins for its maintenance and expression (Rackham *et al.* 2012).

Mitochondrial dysfunction is associated with a wide variety of genetic and degenerative diseases. Robust mitochondrial function is supported by physical exercise and caloric balance, and is central for sustained metabolic health throughout life. Therefore, a more consistent presentation of mitochondrial physiology will improve our understanding of the etiology of disease, the diagnostic repertoire of mitochondrial medicine, with a focus on protective medicine, lifestyle and healthy aging.

Abbreviation: mt, as generally used in mtDNA. Mitochondrion is singular and mitochondria is plural.

1. Introduction

Mitochondria are the powerhouses of the cell with numerous physiological, molecular, and genetic functions (**Box 1**). Every study of mitochondrial health and disease is faced with **E**volution, **A**ge, **G**ender and sex, **L**ifestyle, and **E**nvironment (EAGLE) as essential background conditions intrinsic to the individual patient or subject, cohort, species, tissue and to some extent even cell line. As a large and coordinated group of laboratories and researchers, the mission of the global MitoEAGLE Network is to generate the necessary scale, type, and quality of consistent data sets and conditions to address this intrinsic complexity. Harmonization of experimental protocols and implementation of a quality control and data management system are required to interrelate results gathered across a spectrum of studies and to generate a rigorously monitored database focused on mitochondrial respiratory function. In this way, researchers within the same and across different disciplines can compare findings across traditions and generations to clearly defined and accepted international standards.

Reliability and comparability of quantitative results depend on the accuracy of measurements under strictly-defined conditions. A conceptual framework is required to warrant meaningful interpretation and comparability of experimental outcomes carried out by research groups at different institutes. With an emphasis on quality of research, collected data can be useful far beyond the specific question of a particular experiment. Enabling meta-analytic studies is the most economic way of providing robust answers to biological questions (Cooper *et al.* 2009). Vague or ambiguous jargon can lead to confusion and may relegate valuable signals to wasteful noise. For this reason, measured values must be expressed in standard units for each parameter used to define mitochondrial respiratory function. Harmonization of nomenclature and definition of technical terms are essential to improve the awareness of the intricate meaning of current and past scientific vocabulary, for documentation and integration into databases in general, and quantitative modelling in particular (Beard 2005). The focus on coupling states and fluxes through metabolic pathways of aerobic energy transformation in mitochondrial preparations is a first step in the attempt to generate a conceptually-oriented nomenclature in bioenergetics and mitochondrial physiology. Coupling states of intact cells, the protonmotive force, and respiratory control by fuel substrates and specific inhibitors of respiratory enzymes will be reviewed in subsequent communications.

2. Oxidative phosphorylation and coupling states in mitochondrial preparations

> '*Every professional group develops its own technical jargon for talking about matters of critical concern ... People who know a word can share that idea with other members of their group, and a shared vocabulary is part of the glue that holds people together and allows them to create a shared culture*' (Miller 1991).

Mitochondrial preparations are defined as either isolated mitochondria, or tissue and cellular preparations in which the barrier function of the plasma membrane is disrupted. Since this entails the loss of cell viability, mitochondrial preparations are not studied *in vivo*. In contrast to isolated mitochondria and tissue homogenate preparations, mitochondria in permeabilized tissues and cells are *in situ* relative to the plasma membrane. The plasma membrane separates the intracellular compartment including the cytosol, nucleus, and organelles from the environment of the cell. The plasma membrane consists of a lipid bilayer with embedded proteins and attached organic molecules that collectively control the selective permeability of ions, organic molecules, and particles across the cell boundary. The intact plasma membrane prevents the passage of many water-soluble mitochondrial substrates and inorganic ions—such as succinate, adenosine diphosphate (ADP) and inorganic phosphate (P_i), that must be controlled at kinetically-saturating concentrations for the analysis of respiratory

capacities; this limits the scope of investigations into mitochondrial respiratory function in intact cells (**Figure 2**).

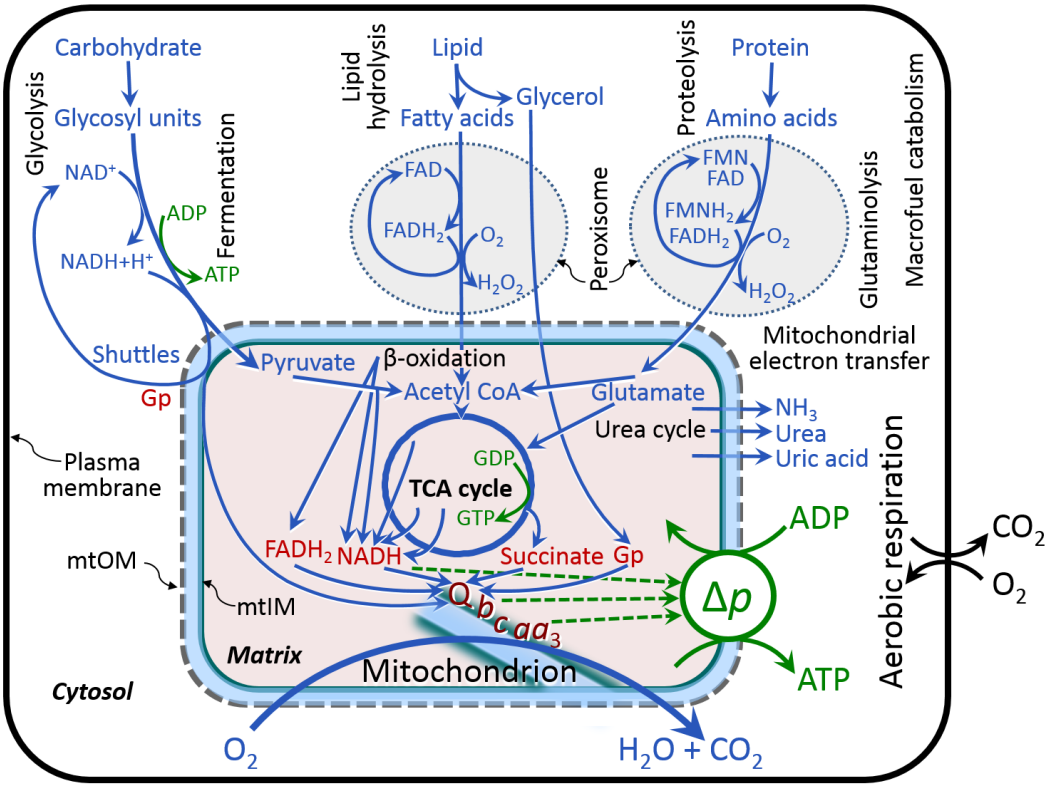

Figure 2. Mitochondrial respiration in the framework of cellular catabolism
Mitochondrial respiration is the utilization of fuel substrates for electron transfer to O_2 as the electron acceptor. Mitochondrial fuel substrates are the products of extra-mitochondrial catabolism of macrofuels or are taken up by the cell as small molecules. Many fuel substrates are catabolized to acetyl-CoA or glutamate, and further electron transfer reduces nicotinamide adenine dinucleotide to NADH or flavin adenine dinucleotide to $FADH_2$. In aerobic respiration, electron transfer is coupled to the phosphorylation of ADP to ATP, with energy transformation mediated by the protonmotive force, Δp. Anabolic reactions are linked to catabolism, both by ATP as the intermediary energy currency and by small organic precursor molecules as building blocks for biosynthesis (not shown). Glycolysis involves substrate-level phosphorylation of ADP to ATP in fermentation without utilization of O_2. In contrast, extra-mitochondrial oxidation of fatty acids and amino acids proceeds partially in peroxisomes without coupling to ATP production: acyl-CoA oxidase catalyzes the oxidation of $FADH_2$ with electron transfer to O_2; amino acid oxidases oxidize flavin mononucleotide $FMNH_2$ or $FADH_2$. Coenzyme Q, Q, and the cytochromes *b*, *c*, and aa_3 are redox systems of the mitochondrial inner membrane, mtIM. Dashed arrows indicate the connection between the redox proton pumps (respiratory Complexes CI, CIII and CIV) and the transmembrane Δp. Mitochondrial outer membrane, mtOM; glycerol-3-phosphate, Gp; tricarboxylic acid cycle, TCA cycle.

The cholesterol content of the plasma membrane is high compared to mitochondrial membranes. Therefore, mild detergents—such as digitonin and saponin—can be applied to selectively permeabilize the plasma membrane by interaction with cholesterol and allow free exchange of organic molecules and inorganic ions between the cytosol and the immediate cell environment, while maintaining the integrity and localization of organelles, cytoskeleton, and the nucleus. Application of optimum concentrations of permeabilization agents (mild detergents or toxins) leads to washout of cytosolic marker enzymes—such as lactate dehydrogenase—and results in the complete loss of cell viability, tested by nuclear staining using membrane-

impermeable dyes, while mitochondrial function remains intact. Respiration of isolated mitochondria remains unaltered after the addition of low concentrations of digitonin or saponin. In addition to mechanical cell disruption during homogenization of tissue, permeabilization agents may be applied to ensure permeabilization of all cells. Suspensions of cells permeabilized in the respiration chamber and crude tissue homogenates contain all components of the cell at highly dilute concentrations. All mitochondria are retained in chemically-permeabilized mitochondrial preparations and crude tissue homogenates. In the preparation of isolated mitochondria, the cells or tissues are homogenized, and the mitochondria are separated from other cell fractions and purified by differential centrifugation, entailing the loss of a fraction of the total mitochondrial content. Typical mitochondrial recovery ranges from 30% to 80%. Maximization of the purity of isolated mitochondria may compromise not only the mitochondrial yield but also the structural and functional integrity. Therefore, protocols to isolate mitochondria need to be optimized according to each study. The term mitochondrial preparation does not include further fractionation of mitochondrial components, neither submitochondrial particles.

2.1. Respiratory control and coupling

Respiratory coupling control states are established in studies of mitochondrial preparations to obtain reference values for various output variables. Physiological conditions *in vivo* deviate from these experimentally obtained states. Since kinetically-saturating concentrations, *e.g.*, of ADP or oxygen (O_2; dioxygen), may not apply to physiological intracellular conditions, relevant information is obtained in studies of kinetic responses to variations in [ADP] or [O_2] in the range between kinetically-saturating concentrations and anoxia (Gnaiger 2001).

The steady-state: Mitochondria represent a thermodynamically open system in non-equilibrium states of biochemical energy transformation. State variables (protonmotive force; redox states) and metabolic *rates* (fluxes) are measured in defined mitochondrial respiratory *states*. Steady-states can be obtained only in open systems, in which changes by *internal* transformations, *e.g.*, O_2 consumption, are instantaneously compensated for by *external* fluxes, *e.g.*, O_2 supply, preventing a change of O_2 concentration in the system (Gnaiger 1993b). Mitochondrial respiratory states monitored in closed systems satisfy the criteria of pseudo-steady states for limited periods of time, when changes in the system (concentrations of O_2, fuel substrates, ADP, P_i, H^+) do not exert significant effects on metabolic fluxes (respiration, phosphorylation). Such pseudo-steady states require respiratory media with sufficient buffering capacity and substrates maintained at kinetically-saturating concentrations, and thus depend on the kinetics of the processes under investigation.

Specification of biochemical dose: Substrates, uncouplers, inhibitors, and other chemical reagents are titrated to dissect mitochondrial function. Nominal concentrations of these substances are usually reported as initial amount of substance concentration [$mol \cdot L^{-1}$] in the incubation medium. When aiming at the measurement of kinetically saturated processes—such as OXPHOS-capacities, the concentrations for substrates can be chosen according to the apparent equilibrium constant, K_m'. In the case of hyperbolic kinetics, only 80% of maximum respiratory capacity is obtained at a substrate concentration of four times the K_m', whereas substrate concentrations of 5, 9, 19 and 49 times the K_m' are theoretically required for reaching 83%, 90%, 95% or 98% of the maximal rate (Gnaiger 2001). Other reagents are chosen to inhibit or alter some processes. The amount of these chemicals in an experimental incubation is selected to maximize effect, avoiding unacceptable off-target consequences that would adversely affect the data being sought. Specifying the amount of substance in an incubation as nominal concentration in the aqueous incubation medium can be ambiguous (Doskey *et al.* 2015), particularly for lipophilic substances (oligomycin, uncouplers, permeabilization agents)

or cations (TPP^+; fluorescent dyes such as safranin, TMRM), which accumulate in biological membranes or in the mitochondrial matrix. For example, a dose of digitonin of 8 fmol·cell^{-1} (10 pg·cell^{-1}; 10 µg·10^{-6} cells) is optimal for permeabilization of endothelial cells, and the concentration in the incubation medium has to be adjusted according to the cell density applied (Doerrier *et al.* 2018).

Generally, dose/exposure can be specified per unit of biological sample, *i.e.*, (nominal moles of xenobiotic)/(number of cells) [mol·cell^{-1}] or, as appropriate, per mass of biological sample [mol·kg^{-1}]. This approach to specification of dose/exposure provides a scalable parameter that can be used to design experiments, help interpret a wide variety of experimental results, and provide absolute information that allows researchers worldwide to make the most use of published data (Doskey *et al.* 2015).

Phosphorylation, P», and P»/O_2 ratio: *Phosphorylation* in the context of OXPHOS is defined as phosphorylation of ADP by P_i to form ATP. On the other hand, the term phosphorylation is used generally in many contexts, *e.g.*, protein phosphorylation. This justifies consideration of a symbol more discriminating and specific than P as used in the P/O ratio (phosphate to atomic oxygen ratio), where P indicates phosphorylation of ADP to ATP or GDP to GTP (**Figure 2**). We propose the symbol P» for the endergonic (uphill) direction of phosphorylation ADP→ATP, and likewise the symbol P« for the corresponding exergonic (downhill) hydrolysis ATP→ADP (**Figure 3**). P» refers mainly to electrontransfer phosphorylation but may also involve substrate-level phosphorylation as part of the tricarboxylic acid (TCA) cycle (succinyl-CoA ligase; phosphoglycerate kinase) and phosphorylation of ADP catalyzed by pyruvate kinase, and of GDP phosphorylated by phosphoenolpyruvate carboxykinase. Transphosphorylation is performed by adenylate kinase, creatine kinase, hexokinase and nucleoside diphosphate kinase. In isolated mammalian mitochondria, ATP production catalyzed by adenylate kinase (2 ADP ↔ ATP + AMP) proceeds without fuel substrates in the presence of ADP (Komlódi and Tretter 2017). Kinase cycles are involved in intracellular energy transfer and signal transduction for regulation of energy flux.

The P»/O_2 ratio (P»/4 e$^-$) is two times the 'P/O' ratio (P»/2 e$^-$) of classical bioenergetics. P»/O_2 is a generalized symbol, not specific for determination of P_i consumption (P_i/O_2 flux ratio), ADP depletion (ADP/O_2 flux ratio), or ATP production (ATP/O_2 flux ratio). The mechanistic P»/O_2 ratio—or P»/O_2 stoichiometry—is calculated from the proton–to–O_2 and proton–to–phosphorylation coupling stoichiometries (**Figure 3A**):

$$P»/O_2 = \frac{H^+_{pos}/O_2}{H^+_{neg}/P»} \quad (1)$$

The H^+_{pos}/O_2 *coupling stoichiometry* (referring to the full 4 electron reduction of O_2) depends on the ET-pathway control state, which defines the relative involvement of the three coupling sites (CI, CIII and CIV) in the catabolic pathway of electrons to O_2. This varies with: (*1*) a bypass of CI by single or multiple electron input into the Q-junction; and (*2*) a bypass of CIV by involvement of alternative oxidases, AOX, which are not expressed in mammalian mitochondria.

H^+_{pos}/O_2 is 12 in the ET-pathways involving CIII and CIV as proton pumps, increasing to 20 for the NADH-pathway (**Figure 3A**), but a general consensus on H^+_{pos}/O_2 stoichiometries remains to be reached (Hinkle 2005; Wikström and Hummer 2012; Sazanov 2015). The H^+_{neg}/P» coupling stoichiometry (3.7; **Figure 3A**) is the sum of 2.7 H^+_{neg} required by the F-ATPase of vertebrate and most invertebrate species (Watt *et al.* 2010) and the proton balance in the translocation of ADP, ATP and P_i (**Figure 3B**). Taken together, the mechanistic P»/O_2 ratio is calculated at 5.4 and 3.3 for NADH- and succinate-linked respiration, respectively (Eq. 1). The corresponding classical P»/O ratios (referring to the 2 electron reduction of 0.5 O_2) are 2.7 and 1.6 (Watt *et al.* 2010), in agreement with the measured P»/O ratio for succinate of 1.58 ± 0.02 (Gnaiger *et al.* 2000).

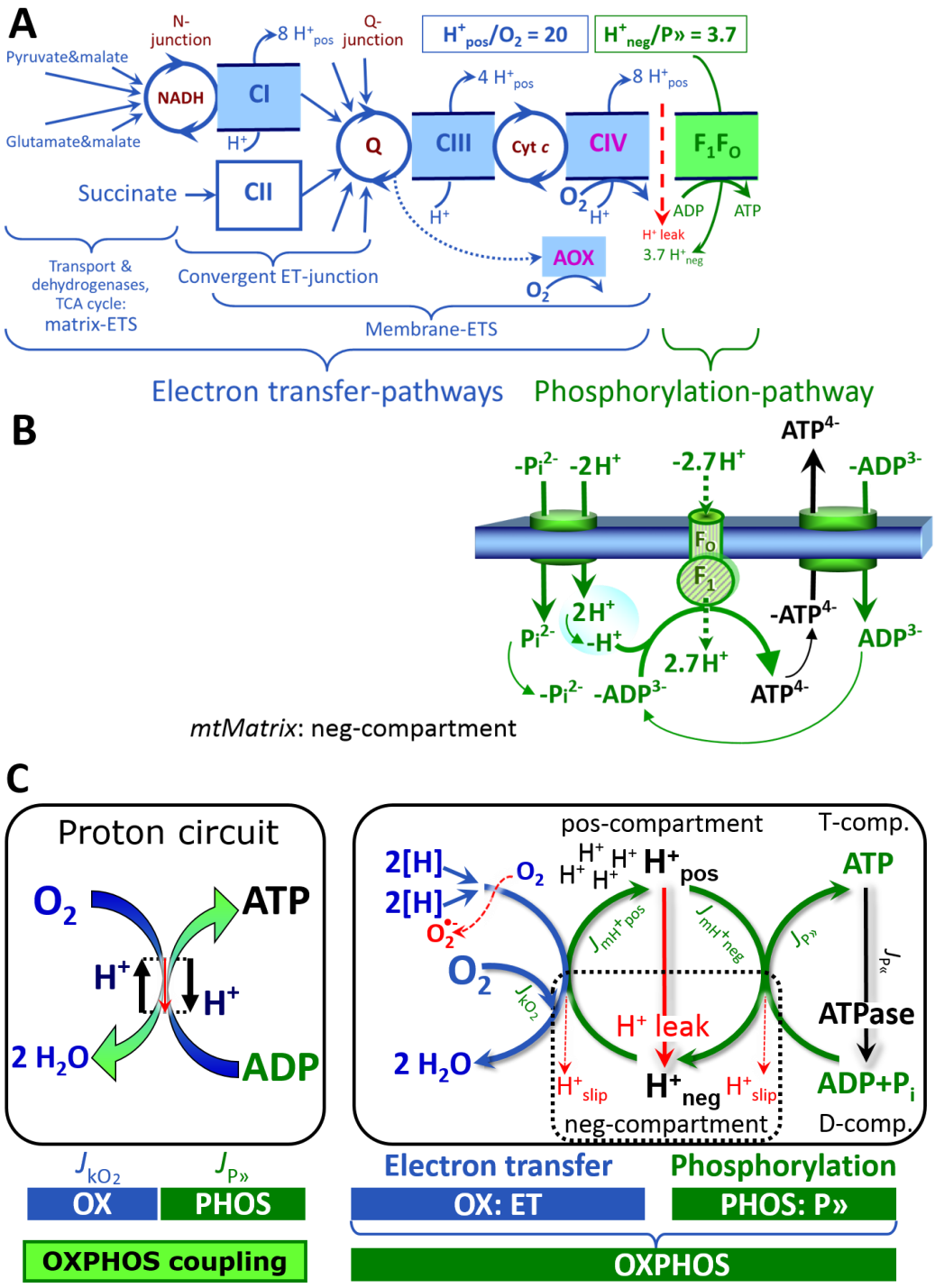

Figure 3. Oxidative phosphorylation (OXPHOS)

(A) The mitochondrial electron transfer system (ETS) is fuelled by diffusion and transport of substrates across the mitochondrial outer and inner membrane and consists of the matrix-ETS and membrane-ETS. ET-pathways are coupled to the phosphorylation-pathway. ET-pathways converge at the N-junction and Q-junction. Additional arrows indicate electron entry into the Q-junction through electron transferring flavoprotein, glycerophosphate dehydrogenase, dihydro-orotate dehydrogenase, choline dehydrogenase, and sulfide-ubiquinone oxidoreductase. The dotted arrow indicates the branched pathway of oxygen consumption by alternative quinol oxidase (AOX). The H^+_{pos}/O_2 ratio is the outward proton flux from the matrix space to the positively (pos) charged vesicular compartment, divided by catabolic O_2 flux in the NADH-pathway. The $H^+_{neg}/P»$ ratio is the inward proton flux from the inter-membrane space

to the negatively (neg) charged matrix space, divided by the flux of phosphorylation of ADP to ATP. These are not fixed stoichiometries due to ion leaks and proton slip.
(**B**) Phosphorylation-pathway catalyzed by the proton pump F_1F_O-ATPase (F-ATPase, ATP synthase), adenine nucleotide translocase, and inorganic phosphate transporter. The $H^+_{neg}/P»$ stoichiometry is the sum of the coupling stoichiometry in the F-ATPase reaction (-2.7 H^+_{pos} from the positive intermembrane space, 2.7 H^+_{neg} to the matrix, *i.e.*, the negative compartment) and the proton balance in the translocation of ADP^{3-}, ATP^{4-} and P_i^{2-}.
(**C**) The proton circuit and coupling in OXPHOS. 2[H] indicates the reduced hydrogen equivalents of fuel substrates of the catabolic reaction k with oxygen. O_2 flux, J_{kO_2}, through the catabolic ET-pathway, is coupled to flux through the phosphorylation-pathway of ADP to ATP, $J_{P»}$. The redox proton pumps of the ET-pathway drive proton flux into the positive (pos) compartment, J_{mH^+pos}, generating the output protonmotive force (motive, subscript m). F-ATPase is coupled to inward proton current into the negative (neg) compartment, J_{mH^+neg}, to phosphorylate ADP+P_i to ATP. The system is defined by the boundaries (full black line) and is not a black box, but is analysed as a compartmental system. The negative compartment (neg–compartment, enclosed by the dotted line) is the matrix space, separated by the mtIM from the positive compartment (pos–compartment). ADP+P_i and ATP are the substrate- and product–compartments (scalar ADP and ATP compartments, D–comp. and T–comp.), respectively. At steady-state proton turnover, $J_{\infty H^+}$, and ATP turnover, $J_{\infty P}$, maintain concentrations constant, when $J_{mH^+\infty} = J_{mH^+pos} = J_{mH^+neg}$, and $J_{P\infty} = J_{P»} = J_{P«}$. Modified from (A) Lemieux *et al*. (2017) and (B,C) Gnaiger (2014).

The effective P»/O_2 flux ratio ($Y_{P»/O_2} = J_{P»}/J_{kO_2}$) is diminished relative to the mechanistic P»/O_2 ratio by intrinsic and extrinsic uncoupling and dyscoupling (**Figure 4**). Such generalized uncoupling is different from switching to mitochondrial pathways that involve fewer than three proton pumps ('coupling sites': Complexes CI, CIII and CIV), bypassing CI through multiple electron entries into the Q-junction, or CIII and CIV through AOX (**Figure 3**). Reprogramming of mitochondrial pathways may be considered as a switch of gears (changing the stoichiometry by altering the substrate that is oxidized) rather than uncoupling (loosening the tightness of coupling relative to a fixed stoichiometry). In addition, $Y_{P»/O_2}$ depends on several experimental conditions of flux control, increasing as a hyperbolic function of [ADP] to a maximum value (Gnaiger 2001).

Control and regulation: The terms metabolic *control* and *regulation* are frequently used synonymously, but are distinguished in metabolic control analysis: 'We could understand the regulation as the mechanism that occurs when a system maintains some variable constant over time, in spite of fluctuations in external conditions (homeostasis of the internal state). On the other hand, metabolic control is the power to change the state of the metabolism in response to an external signal' (Fell 1997). Respiratory control may be induced by experimental control signals that *exert* an influence on: (*1*) ATP demand and ADP phosphorylation-rate; (*2*) fuel substrate composition, pathway competition; (*3*) available amounts of substrates and O_2, *e.g.*, starvation and hypoxia; (*4*) the protonmotive force, redox states, flux–force relationships, coupling and efficiency; (*5*) Ca^{2+} and other ions including H^+; (*6*) inhibitors, *e.g.*, nitric oxide or intermediary metabolites such as oxaloacetate; (*7*) signalling pathways and regulatory proteins, *e.g.*, insulin resistance, transcription factor hypoxia inducible factor 1. *Mechanisms* of respiratory control and regulation include adjustments of: (*1*) enzyme activities by allosteric mechanisms and phosphorylation; (*2*) enzyme content, concentrations of cofactors and conserved moieties—such as adenylates, nicotinamide adenine dinucleotide [NAD^+/NADH], coenzyme Q, cytochrome *c*; (*3*) metabolic channeling by supercomplexes; and *(4)* mitochondrial density (enzyme concentrations and membrane area) and morphology (cristae folding, fission and fusion). Mitochondria are targeted directly by hormones, thereby affecting their energy metabolism (Lee *et al.* 2013; Gerö and Szabo 2016; Price and Dai 2016; Moreno

et al. 2017). Evolutionary or acquired differences in the genetic and epigenetic basis of mitochondrial function (or dysfunction) between subjects and gene therapy; age; gender, biological sex, and hormone concentrations; life style including exercise and nutrition; and environmental issues including thermal, atmospheric, toxicological and pharmacological factors, exert an influence on all control mechanisms listed above. For reviews, see Brown 1992; Gnaiger 1993a, 2009; 2014; Paradies *et al.* 2014; Morrow *et al*. 2017.

Respiratory control and response: Lack of control by a metabolic pathway, *e.g.*, phosphorylation-pathway, means that there will be no response to a variable activating it, *e.g.*, [ADP]. The reverse, however, is not true as the absence of a response to [ADP] does not exclude the phosphorylation-pathway from having some degree of control. The degree of control of a component of the OXPHOS-pathway on an output variable—such as O_2 flux, will in general be different from the degree of control on other outputs—such as phosphorylation-flux or proton leak flux. Therefore, it is necessary to be specific as to which input and output are under consideration (Fell 1997).

Respiratory coupling control and ET-pathway control: Respiratory control refers to the ability of mitochondria to adjust O_2 flux in response to external control signals by engaging various mechanisms of control and regulation. Respiratory control is monitored in a mitochondrial preparation under conditions defined as respiratory states. When phosphorylation of ADP to ATP is stimulated or depressed, an increase or decrease is observed in electron transfer measured as O_2 flux in respiratory coupling states of intact mitochondria ('controlled states' in the classical terminology of bioenergetics). Alternatively, coupling of electron transfer with phosphorylation is disengaged by uncouplers. These protonophores are weak lipid-soluble acids which disrupt the barrier function of the mtIM and thus shortcircuit the protonmotive system, functioning like a clutch in a mechanical system. The corresponding coupling control state is characterized by a high O_2 flux without control by P» ('uncontrolled state').

ET-pathway control states are obtained in mitochondrial preparations by depletion of endogenous substrates and addition to the mitochondrial respiration medium of fuel substrates (2[H] in **Figure 3C**) and specific inhibitors, activating selected mitochondrial catabolic pathways, k (**Figure 3A**). Coupling control states and pathway control states are complementary, since mitochondrial preparations depend on an exogenous supply of pathway-specific fuel substrates and oxygen (Gnaiger 2014).

Coupling: In mitochondrial electron transfer, vectorial transmembrane proton flux is coupled through the redox proton pumps CI, CIII and CIV to the catabolic flux of scalar reactions, collectively measured as O_2 flux (**Figure 3**). Thus mitochondria are elements of energy transformation. Energy is a conserved quantity and cannot be lost or produced in any internal process (First Law of thermodynamics). Open and closed systems can gain or lose energy only by external fluxes—by exchange with the environment. Therefore, energy can neither be produced by mitochondria, nor is there any internal process without energy conservation. Exergy is defined as the Gibbs energy ('free energy') with the potential to perform work under conditions of constant volume and pressure. *Coupling* is the interaction of an exergonic process (spontaneous, negative exergy change) with an endergonic process (positive exergy change) in energy transformations which conserve part of the exergy that would be irreversibly lost or dissipated in an uncoupled process.

Uncoupling: Uncoupling of mitochondrial respiration is a general term comprising diverse mechanisms:

1. Proton leak across the mtIM from the pos– to the neg–compartment (**Figure 3C**);
2. Cycling of other cations, strongly stimulated by permeability transition, or experimentally induced by valinomycin in the presence of K^+;
3. Proton slip in the redox proton pumps when protons are effectively not pumped (CI, CIII and CIV) or are not driving phosphorylation (F-ATPase);

4. Loss of vesicular (compartmental) integrity when electron transfer is acoupled;
5. Electron leak in the loosely coupled univalent reduction of O_2 to superoxide ($O_2^{\bullet-}$; superoxide anion radical).

Differences of terms—uncoupled *vs.* noncoupled—are easily overlooked, although they relate to different meanings of uncoupling (**Figure 4**).

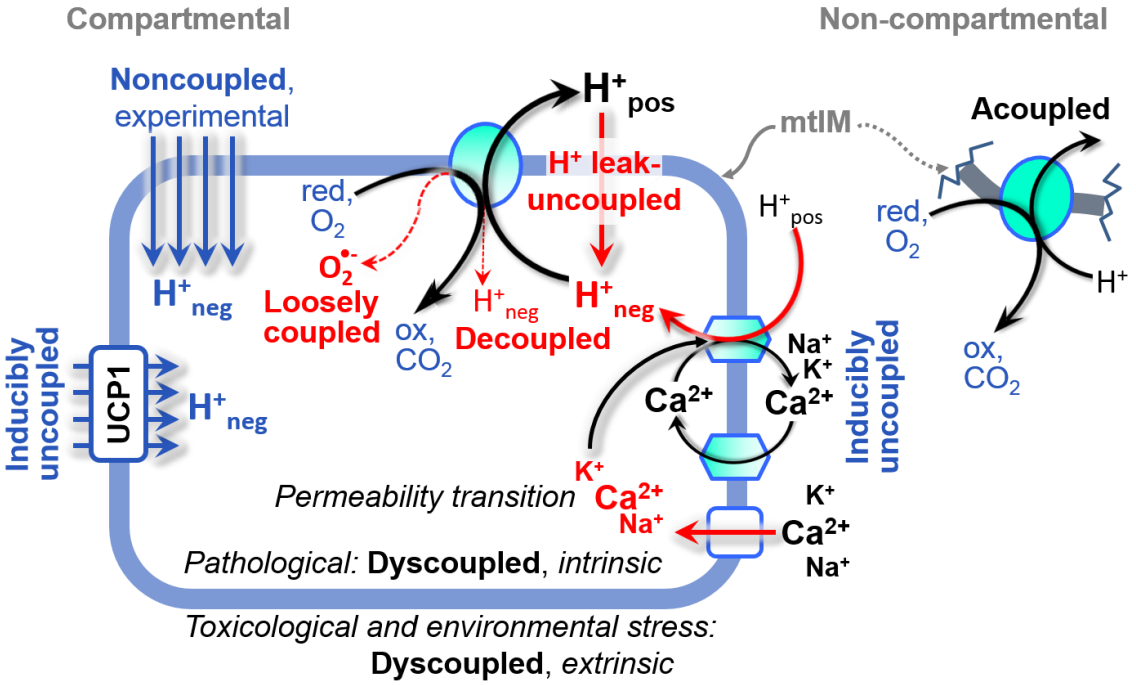

Figure 4. Mechanisms of respiratory uncoupling
An intact mitochondrial inner membrane, mtIM, is required for vectorial, compartmental coupling. 'Acoupled' respiration is the consequence of structural disruption with catalytic activity of non-compartmental mitochondrial fragments. Inducibly uncoupled (activation of UCP1) and experimentally noncoupled respiration (titration of protonophores) stimulate respiration to maximum O_2 flux. H^+ leak-uncoupled, decoupled, and loosely coupled respiration are components of intrinsic uncoupling. Pathological dysfunction may affect all types of uncoupling, including permeability transition, causing intrinsically dyscoupled respiration. Similarly, toxicological and environmental stress factors can cause extrinsically dyscoupled respiration.

2.2. Coupling states and respiratory rates

Respiratory capacities in coupling control states: To extend the classical nomenclature on mitochondrial coupling states (Section 2.3) by a concept-driven terminology that explicitly incorporates information on the meaning of respiratory states, the terminology must be general and not restricted to any particular experimental protocol or mitochondrial preparation (Gnaiger 2009). Concept-driven nomenclature aims at mapping the *meaning and concept behind* the words and acronyms onto the *forms* of words and acronyms (Miller 1991). The focus of concept-driven nomenclature is primarily the conceptual 'why', along with clarification of the experimental 'how'. Respiratory capacities delineate, comparable to channel capacity in information theory (Schneider 2006), the upper bound of the rate of respiration measured in defined coupling control states and electron transfer-pathway (ET-pathway) states (**Figure 5**).

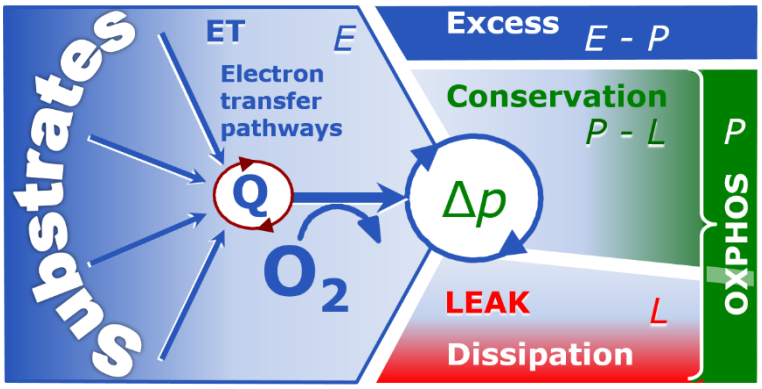

Figure 5. Four-compartment model of oxidative phosphorylation Respiratory states (ET, OXPHOS, LEAK; **Table 1**) and corresponding rates (*E*, *P*, *L*) are connected by the protonmotive force, Δp. ET-capacity, *E* (*1*), is partitioned into (*2*) dissipative LEAK-respiration, *L*, when the Gibbs energy change of catabolic O_2 flux is irreversibly lost, (*3*) net OXPHOS-capacity, *P*-*L*, with partial conservation of the capacity to perform work, and (*4*) the excess capacity, *E*-*P*. Modified from Gnaiger (2014).

Table 1. Coupling states and residual oxygen consumption in mitochondrial preparations in relation to respiration- and phosphorylation-flux, J_{kO_2} and $J_{P\text{»}}$, and protonmotive force, Δp. Coupling states are established at kinetically-saturating concentrations of fuel substrates and O_2.

State	J_{kO_2}	$J_{P\text{»}}$	Δp	Inducing factors	Limiting factors
LEAK	*L*; low, cation leak-dependent respiration	0	max.	proton leak, slip, and cation cycling	$J_{P\text{»}} = 0$: (*1*) without ADP, L_N; (*2*) max. ATP/ADP ratio, L_T; or (*3*) inhibition of the phosphorylation-pathway, L_{Omy}
OXPHOS	*P*; high, ADP-stimulated respiration	max.	high	kinetically-saturating [ADP] and [P_i]	$J_{P\text{»}}$ by phosphorylation-pathway; or J_{kO_2} by ET-capacity
ET	*E*; max., noncoupled respiration	0	low	optimal external uncoupler concentration for max. $J_{O_2,E}$	J_{kO_2} by ET-capacity
ROX	*Rox*; min., residual O_2 consumption	0	0	$J_{O_2,Rox}$ in non-ET-pathway oxidation reactions	inhibition of all ET-pathways; or absence of fuel substrates

To provide a diagnostic reference for respiratory capacities of core energy metabolism, the capacity of *oxidative phosphorylation*, OXPHOS, is measured at kinetically-saturating concentrations of ADP and P_i. The *oxidative* ET-capacity reveals the limitation of OXPHOS-capacity mediated by the *phosphorylation*-pathway. The ET- and phosphorylation-pathways comprise coupled segments of the OXPHOS-system. ET-capacity is measured as noncoupled respiration by application of *external uncouplers*. The contribution of *intrinsically uncoupled* O_2 consumption is studied by preventing the stimulation of phosphorylation either in the absence of ADP or by inhibition of the phosphorylation-pathway. The corresponding states are collectively classified as LEAK-states, when O_2 consumption compensates mainly for ion leaks, including the proton leak. Defined coupling states are induced by: (*1*) adding cation chelators such as EGTA, binding free Ca^{2+} and thus limiting cation cycling; (*2*) adding ADP and P_i; (*3*) inhibiting the phosphorylation-pathway; and (*4*) uncoupler titrations, while

maintaining a defined ET-pathway state with constant fuel substrates and inhibitors of specific branches of the ET-pathway (**Figure 5**).

The three coupling states, ET, LEAK and OXPHOS, are shown schematically with the corresponding respiratory rates, abbreviated as *E*, *L* and *P*, respectively (**Figure 5**). We distinguish metabolic *pathways* from metabolic *states* and the corresponding metabolic *rates*; for example: ET-pathways (**Figure 5**), ET-states (**Figure 6C**), and ET-capacities, *E*, respectively (**Table 1**). The protonmotive force is *high* in the OXPHOS-state when it drives phosphorylation, *maximum* in the LEAK-state of coupled mitochondria, driven by LEAK-respiration at a minimum back flux of cations to the matrix side, and *very low* in the ET-state when uncouplers short-circuit the proton cycle (**Table 1**).

LEAK-state (**Figure 6A**): The LEAK-state is defined as a state of mitochondrial respiration when O_2 flux mainly compensates for ion leaks in the absence of ATP synthesis, at kinetically-saturating concentrations of O_2 and respiratory fuel substrates. LEAK-respiration is measured to obtain an estimate of *intrinsic uncoupling* without addition of an experimental uncoupler: (*1*) in the absence of adenylates, *i.e.*, AMP, ADP and ATP; (*2*) after depletion of ADP at a maximum ATP/ADP ratio; or (*3*) after inhibition of the phosphorylation-pathway by inhibitors of F-ATPase—such as oligomycin, or of adenine nucleotide translocase—such as carboxyatractyloside. Adjustment of the nominal concentration of these inhibitors to the density of biological sample applied can minimize or avoid inhibitory side-effects exerted on ET-capacity or even some dyscoupling.

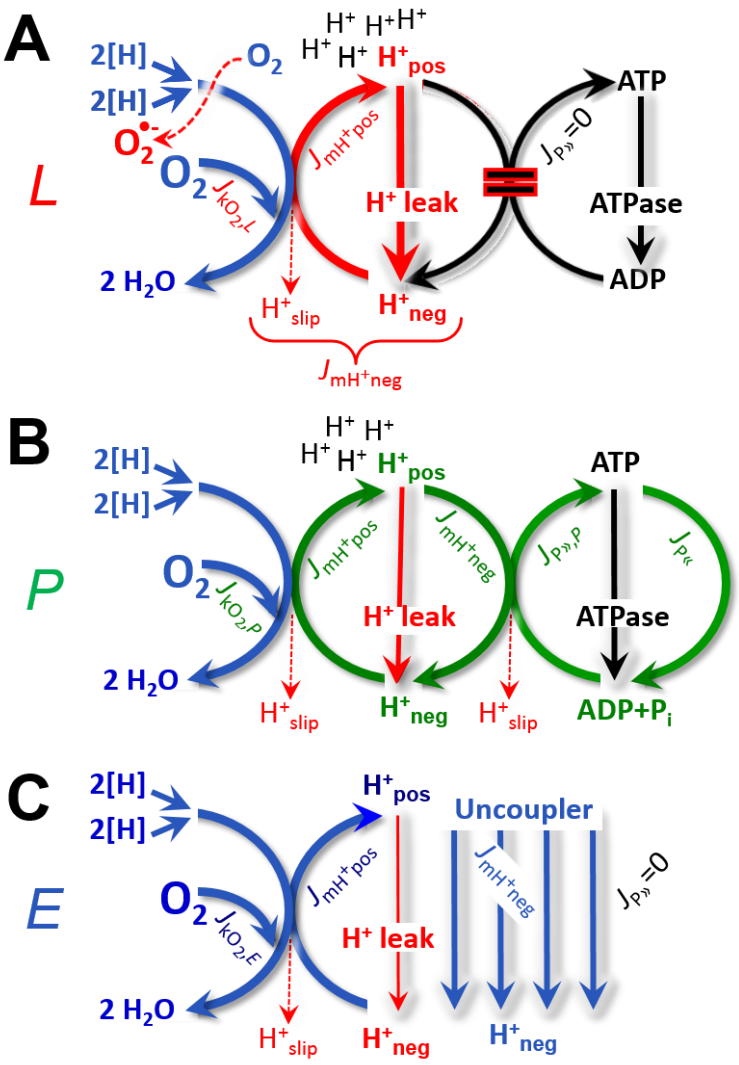

Figure 6. Respiratory coupling states
(A) LEAK-state and rate, *L*: Phosphorylation is arrested, $J_{P»} = 0$, and catabolic O_2 flux, $J_{kO_2,L}$, is controlled mainly by the proton leak, $J_{mH^+neg,L}$, at maximum protonmotive force (**Figure 4**).
(B) OXPHOS-state and rate, *P*: Phosphorylation, $J_{P»}$, is stimulated by kinetically-saturating [ADP] and [P_i], and is supported by a high protonmotive force. O_2 flux, $J_{kO_2,P}$, is well-coupled at a P»/O_2 ratio of $J_{P»,P}/J_{O_2,P}$.
(C) ET-state and rate, *E*: Noncoupled respiration, $J_{kO2,E}$, is maximum at optimum exogenous uncoupler concentration and phosphorylation is zero, $J_{P»} = 0$. See also **Figure 3**.

Proton leak and uncoupled respiration: Proton leak is a leak current of protons. The intrinsic proton leak is the *uncoupled* process in which protons diffuse across the mtIM in the dissipative direction of the downhill protonmotive force without coupling to phosphorylation (**Figure 6A**). The proton leak flux depends non-linearly on the protonmotive force (Garlid *et al.* 1989; Divakaruni and Brand 2011), it is a property of the mtIM and may be enhanced due to possible contaminations by free fatty acids. Inducible uncoupling mediated by uncoupling protein 1 (UCP1) is physiologically controlled, *e.g.*, in brown adipose tissue. UCP1 is a member of the mitochondrial carrier family which is involved in the translocation of protons across the mtIM (Klingenberg 2017). Consequently, the short-circuit diminishes the protonmotive force and stimulates electron transfer to O_2 and heat dissipation without phosphorylation of ADP.

Cation cycling: There can be other cation contributors to leak current including calcium and probably magnesium. Calcium current is balanced by mitochondrial Na^+/Ca^{2+} exchange, which is balanced by Na^+/H^+ or K^+/H^+ exchanges. This is another effective uncoupling mechanism different from proton leak (**Table 2**).

Table 2. Terms on respiratory coupling and uncoupling.

Term		J_{kO_2}	P»/O_2	Note
acoupled			0	electron transfer in mitochondrial fragments without vectorial proton translocation (**Figure 4**)
intrinsic, no protonophore added	uncoupled	*L*	0	non-phosphorylating LEAK-respiration (**Figure 6A**)
	proton leak-uncoupled		0	component of *L*, H^+ diffusion across the mtIM (**Figure 4**)
	decoupled		0	component of *L*, proton slip (**Figure 4**)
	loosely coupled		0	component of *L*, lower coupling due to superoxide formation and bypass of proton pumps (**Figure 4**)
	dyscoupled		0	pathologically, toxicologically, environmentally increased uncoupling, mitochondrial dysfunction
	inducibly uncoupled		0	by UCP1 or cation (*e.g.*, Ca^{2+}) cycling (**Figure 4**)
noncoupled		*E*	0	non-phosphorylating respiration stimulated to maximum flux at optimum exogenous uncoupler concentration (**Figure 6C**)
well-coupled		*P*	high	phosphorylating respiration with an intrinsic LEAK component (**Figure 6B**)
fully coupled		*P* – *L*	max.	OXPHOS-capacity corrected for LEAK-respiration (**Figure 5**)

Proton slip and decoupled respiration: Proton slip is the *decoupled* process in which protons are only partially translocated by a redox proton pump of the ET-pathways and slip back to the original vesicular compartment. The proton leak is the dominant contributor to the overall leak current in mammalian mitochondria incubated under physiological conditions at 37 °C, whereas proton slip is increased at lower experimental temperature (Canton *et al.* 1995). Proton slip can also happen in association with the F-ATPase, in which the proton slips downhill across the pump to the matrix without contributing to ATP synthesis. In each case, proton slip is a property of the proton pump and increases with the pump turnover rate.

Electron leak and loosely coupled respiration: Superoxide production by the ETS leads to a bypass of redox proton pumps and correspondingly lower P»/O_2 ratio. This depends on the actual site of electron leak and the scavenging of hydrogen peroxide by cytochrome *c*, whereby electrons may re-enter the ETS with proton translocation by CIV.

Loss of compartmental integrity and acoupled respiration: Electron transfer and catabolic O_2 flux proceed without compartmental proton translocation in disrupted mitochondrial fragments. Such fragments form during mitochondrial isolation, and may not fully fuse to re-establish structurally intact mitochondria. Loss of mtIM integrity, therefore, is the cause of acoupled respiration, which is a nonvectorial dissipative process without control by the protonmotive force.

Dyscoupled respiration: Mitochondrial injuries may lead to *dyscoupling* as a pathological or toxicological cause of *uncoupled* respiration. Dyscoupling may involve any type of uncoupling mechanism, *e.g.*, opening the permeability transition pore. Dyscoupled respiration is distinguished from the experimentally induced *noncoupled* respiration in the ET-state (**Table 2**).

OXPHOS-state (**Figure 6B**): The OXPHOS-state is defined as the respiratory state with kinetically-saturating concentrations of O_2, respiratory and phosphorylation substrates, and absence of exogenous uncoupler, which provides an estimate of the maximal respiratory capacity in the OXPHOS-state for any given ET-pathway state. Respiratory capacities at kinetically-saturating substrate concentrations provide reference values or upper limits of performance, aiming at the generation of data sets for comparative purposes. Physiological activities and effects of substrate kinetics can be evaluated relative to the OXPHOS-capacity.

As discussed previously, 0.2 mM ADP does not fully saturate flux in isolated mitochondria (Gnaiger 2001; Puchowicz *et al.* 2004); greater ADP concentration is required, particularly in permeabilized muscle fibres and cardiomyocytes, to overcome limitations by intracellular diffusion and by the reduced conductance of the mtOM (Jepihhina *et al.* 2011, Illaste *et al.* 2012, Simson *et al*. 2016), either through interaction with tubulin (Rostovtseva *et al.* 2008) or other intracellular structures (Birkedal *et al*. 2014). In permeabilized muscle fibre bundles of high respiratory capacity, the apparent K_m for ADP increases up to 0.5 mM (Saks *et al.* 1998), consistent with experimental evidence that >90% saturation is reached only at >5 mM ADP (Pesta and Gnaiger 2012). Similar ADP concentrations are also required for accurate determination of OXPHOS-capacity in human clinical cancer samples and permeabilized cells (Klepinin *et al.* 2016; Koit *et al.* 2017). Whereas 2.5 to 5 mM ADP is sufficient to obtain the actual OXPHOS-capacity in many types of permeabilized tissue and cell preparations, experimental validation is required in each specific case.

Electron transfer-state (**Figure 6C**): The ET-state is defined as the *noncoupled* state with kinetically-saturating concentrations of O_2, respiratory substrate and optimum *exogenous* uncoupler concentration for maximum O_2 flux. O_2 flux determined in the ET-state yields an estimate of ET-capacity. Inhibition of respiration is observed above optimum uncoupler concentrations. As a consequence of the nearly collapsed protonmotive force, the driving force is insufficient for phosphorylation, and $J_{P»} = 0$.

ROX state and *Rox*: Besides the three fundamental coupling states of mitochondrial preparations, the state of residual O_2 consumption, ROX, is relevant to assess respiratory function (**Figure 1**). ROX is not a coupling state. The rate of residual oxygen consumption, *Rox*, is defined as O_2 consumption due to oxidative reactions measured after inhibition of ET—with rotenone, malonic acid and antimycin A. Cyanide and azide inhibit not only CIV but catalase and several peroxidases involved in *Rox*. However, high concentrations of antimycin A, but not rotenone or cyanide, inhibit peroxisomal acyl-CoA oxidase and D-amino acid oxidase (Vamecq *et al.* 1987). ROX represents a baseline that is used to correct respiration measured in defined coupling states. *Rox*-corrected *L*, *P* and *E* not only lower the values of total fluxes, but also changes the flux control ratios *L*/*P* and *L*/*E*. *Rox* is not necessarily equivalent

to non-mitochondrial reduction of O_2, considering O_2-consuming reactions in mitochondria that are not related to ET—such as O_2 consumption in reactions catalyzed by monoamine oxidases (type A and B), monooxygenases (cytochrome P450 monooxygenases), dioxygenase (sulfur dioxygenase and trimethyllysine dioxygenase), and several hydoxylases. Even isolated mitochondrial fractions, especially those obtained from liver, may be contaminated by peroxisomes. This fact makes the exact determination of mitochondrial O_2 consumption and mitochondria-associated generation of reactive oxygen species complicated (Schönfeld *et al.* 2009; Speijer 2016; **Figure 2**). The dependence of ROX-linked O_2 consumption needs to be studied in detail together with non-ET enzyme activities, availability of specific substrates, O_2 concentration, and electron leakage leading to the formation of reactive oxygen species.

Quantitative relations: *E* may exceed or be equal to *P*. $E > P$ is observed in many types of mitochondria, varying between species, tissues and cell types (Gnaiger 2009). *E-P* is the excess ET-capacity pushing the phosphorylation-flux (**Figure 3B**) to the limit of its *capacity of utilizing* the protonmotive force. In addition, the magnitude of *E-P* depends on the tightness of respiratory coupling or degree of uncoupling, since an increase of *L* causes *P* to increase towards the limit of *E*. The *excess E-P* capacity, *E-P*, therefore, provides a sensitive diagnostic indicator of specific injuries of the phosphorylation-pathway, under conditions when *E* remains constant but *P* declines relative to controls (**Figure 5**). Substrate cocktails supporting simultaneous convergent electron transfer to the Q-junction for reconstitution of TCA cycle function establish pathway control states with high ET-capacity, and consequently increase the sensitivity of the *E-P* assay.

E cannot theoretically be lower than *P*. $E < P$ must be discounted as an artefact, which may be caused experimentally by: (*1*) loss of oxidative capacity during the time course of the respirometric assay, since *E* is measured subsequently to *P*; (*2*) using insufficient uncoupler concentrations; (*3*) using high uncoupler concentrations which inhibit ET (Gnaiger 2008); (*4*) high oligomycin concentrations applied for measurement of *L* before titrations of uncoupler, when oligomycin exerts an inhibitory effect on *E*. On the other hand, the excess ET-capacity is overestimated if non-saturating [ADP] or [P_i] are used. See State 3 in the next section.

The net OXPHOS-capacity is calculated by subtracting *L* from *P* (**Figure 5**). The net P»/O_2 equals P»/(*P-L*), wherein the dissipative LEAK component in the OXPHOS-state may be overestimated. This can be avoided by measuring LEAK-respiration in a state when the protonmotive force is adjusted to its slightly lower value in the OXPHOS-state—by titration of an ET inhibitor (Divakaruni and Brand 2011). Any turnover-dependent components of proton leak and slip, however, are underestimated under these conditions (Garlid *et al.* 1993). In general, it is inappropriate to use the term *ATP production* or *ATP turnover* for the difference of O_2 flux measured in the OXPHOS and LEAK states. *P-L* is the upper limit of OXPHOS-capacity that is freely available for ATP production (corrected for LEAK-respiration) and is fully coupled to phosphorylation with a maximum mechanistic stoichiometry (**Figure 5**).

The rates of LEAK respiration and OXPHOS capacity depend on (*1*) the tightness of coupling under the influence of the respiratory uncoupling mechanisms (**Figure 4**), and (*2*) the coupling stoichiometry which varies as a function of the substrate type undergoing oxidation in ET-pathways with either two or three coupling sites (**Figure 3A**). When cocktails with NADH-linked substrates and succinate are used, the relative contribution of ET-pathways with three or two coupling sites cannot be controlled experimentally, is difficult to determine, and may shift in transitions between LEAK-, OXPHOS- and ET-states (Gnaiger 2014). Under these experimental conditions, we cannot separate the tightness of coupling *versus* coupling stoichiometry as the mechanisms of respiratory control in the shift of *L*/*P* ratios. The tightness of coupling and fully coupled O_2 flux, *P-L* (**Table 2**), therefore, are obtained from measurements of coupling control of LEAK respiration, OXPHOS- and ET-capacities in well defined pathway states, using either pyruvate and malate as substrates or the classical succinate and rotenone substrate-inhibitor combination (**Figure 3A**).

2.3. Classical terminology for isolated mitochondria

'When a code is familiar enough, it ceases appearing like a code; one forgets that there is a decoding mechanism. The message is identical with its meaning' (Hofstadter 1979).

Chance and Williams (1955; 1956) introduced five classical states of mitochondrial respiration and cytochrome redox states. **Table 3** shows a protocol with isolated mitochondria in a closed respirometric chamber, defining a sequence of respiratory states. States and rates are not specifically distinguished in this nomenclature.

State 1 is obtained after addition of isolated mitochondria to air-saturated isoosmotic/isotonic respiration medium containing P_i, but no fuel substrates and no adenylates, *i.e.*, AMP, ADP, ATP.

Table 3. Metabolic states of mitochondria (Chance and Williams, 1956; Table V).

State	$[O_2]$	ADP level	Substrate level	Respiration rate	Rate-limiting substance
1	>0	low	low	slow	ADP
2	>0	high	~0	slow	substrate
3	>0	high	high	fast	respiratory chain
4	>0	low	high	slow	ADP
5	0	high	high	0	oxygen

State 2 is induced by addition of a 'high' concentration of ADP (typically 100 to 300 µM), which stimulates respiration transiently on the basis of endogenous fuel substrates and phosphorylates only a small portion of the added ADP. State 2 is then obtained at a low respiratory activity limited by exhausted endogenous fuel substrate availability (**Table 3**). If addition of specific inhibitors of respiratory complexes—such as rotenone—does not cause a further decline of O_2 flux, State 2 is equivalent to the ROX state (See below.). If inhibition is observed, undefined endogenous fuel substrates are a confounding factor of pathway control, contributing to the effect of subsequently externally added substrates and inhibitors. In contrast to the original protocol, an alternative sequence of titration steps is frequently applied, in which the alternative 'State 2' has an entirely different meaning, when this second state is induced by addition of fuel substrate without ADP (LEAK-state; in contrast to State 2 defined in **Table 1** as a ROX state), followed by addition of ADP.

State 3 is the state stimulated by addition of fuel substrates while the ADP concentration is still high (**Table 3**) and supports coupled energy transformation through oxidative phosphorylation. 'High ADP' is a concentration of ADP specifically selected to allow the measurement of State 3 to State 4 transitions of isolated mitochondria in a closed respirometric chamber. Repeated ADP titration re-establishes State 3 at 'high ADP'. Starting at O_2 concentrations near air-saturation (ca. 200 µM O_2 at sea level and 37 °C), the total ADP concentration added must be low enough (typically 100 to 300 µM) to allow phosphorylation to ATP at a coupled O_2 flux that does not lead to O_2 depletion during the transition to State 4. In contrast, kinetically-saturating ADP concentrations usually are 10-fold higher than 'high ADP', *e.g.*, 2.5 mM in isolated mitochondria. The abbreviation State 3u is occasionally used in bioenergetics, to indicate the state of respiration after titration of an uncoupler, without sufficient emphasis on the fundamental difference between OXPHOS-capacity (*well-coupled* with an *endogenous* uncoupled component) and ET-capacity (*noncoupled*).

State 4 is a LEAK-state that is obtained only if the mitochondrial preparation is intact and well-coupled. Depletion of ADP by phosphorylation to ATP causes a decline of O_2 flux in the transition from State 3 to State 4. Under the conditions of State 4, a maximum protonmotive

force and high ATP/ADP ratio are maintained. The gradual decline of $Y_{P»/O_2}$ towards diminishing [ADP] at State 4 must be taken into account for calculation of P»/O_2 ratios (Gnaiger 2001). State 4 respiration, L_T (**Table 1**), reflects intrinsic proton leak and ATP hydrolysis activity. O_2 flux in State 4 is an overestimation of LEAK-respiration if the contaminating ATP hydrolysis activity recycles some ATP to ADP, $J_{P«}$, which stimulates respiration coupled to phosphorylation, $J_{P»} > 0$. This can be tested by inhibition of the phosphorylation-pathway using oligomycin, ensuring that $J_{P»} = 0$ (State 4o). Alternatively, sequential ADP titrations re-establish State 3, followed by State 3 to State 4 transitions while sufficient O_2 is available. Anoxia may be reached, however, before exhaustion of ADP (State 5).

State 5 is the state after exhaustion of O_2 in a closed respirometric chamber. Diffusion of O_2 from the surroundings into the aqueous solution may be a confounding factor preventing complete anoxia (Gnaiger 2001). Chance and Williams (1955) provide an alternative definition of State 5, which gives it the different meaning of ROX versus anoxia: 'State 5 may be obtained by antimycin A treatment or by anaerobiosis'.

In **Table 3**, only States 3 and 4 (and 'State 2' in the alternative protocol: addition of fuel substrates without ADP; not included in the table) are coupling control states, with the restriction that O_2 flux in State 3 may be limited kinetically by non-saturating ADP concentrations (**Table 1**).

3. Normalization: fluxes and flows

3.1. Normalization: system or sample

The term *rate* is not sufficiently defined to be useful for reporting data (**Figure 7**). The inconsistency of the meanings of rate becomes fully apparent when considering Galileo Galilei's famous principle, that 'bodies of different weight all fall at the same rate (have a constant acceleration)' (Coopersmith 2010).

Flow per system, *I*: In a generalization of electrical terms, flow as an extensive quantity (*I*; per system) is distinguished from flux as a size-specific quantity (*J*; per system size) (**Figure 7A**). Electric current is flow, I_{el} [$A \equiv C \cdot s^{-1}$] per system (extensive quantity). When dividing this extensive quantity by system size (cross-sectional area of a 'wire'), a size-specific quantity is obtained, which is flux (current density), $\boldsymbol{J}_{el}$ [$A \cdot m^{-2} = C \cdot s^{-1} \cdot m^{-2}$] (**Box 2**).

Extensive quantities: An extensive quantity increases proportionally with system size. The magnitude of an extensive quantity is completely additive for non-interacting subsystems—such as mass or flow expressed per defined system. The magnitude of these quantities depends on the extent or size of the system (Cohen *et al.* 2008).

Size-specific quantities: 'The adjective *specific* before the name of an extensive quantity is often used to mean *divided by mass*' (Cohen *et al.* 2008). In this system-paradigm, mass-specific flux is flow divided by mass of the *system* (the total mass of everything within the measuring chamber or reactor). A mass-specific quantity is independent of the extent of non-interacting homogenous subsystems. Tissue-specific quantities (related to the *sample* in contrast to the *system*) are of fundamental interest in the field of comparative mitochondrial physiology, where *specific* refers to the *type of the sample* rather than *mass of the system*. The term *specific*, therefore, must be clarified; *sample*-specific, *e.g.*, muscle mass-specific normalization, is distinguished from *system*-specific quantities (mass or volume; **Figure 7**).

Box 2: Metabolic fluxes and flows: vectorial and scalar

Fluxes are *vectors*, if they have *spatial* geometric direction in addition to magnitude. Electric charge per unit time is electric flow or current, $I_{el} = dQ_{el} \cdot dt^{-1}$ [A]. When expressed per

unit cross-sectional area, A [m^2], a vector flux is obtained, which is current density (surface-density of flow) perpendicular to the direction of flux, $\boldsymbol{J}_{el} = I_{el} \cdot A^{-1}$ [$A \cdot m^{-2}$] (Cohen et al. 2008). For all transformations *flows*, I_{tr}, are defined as extensive quantities. Vector and scalar *fluxes* are obtained as $\boldsymbol{J}_{tr} = I_{tr} \cdot A^{-1}$ [$mol \cdot s^{-1} \cdot m^{-2}$] and $J_{tr} = I_{tr} \cdot V^{-1}$ [$mol \cdot s^{-1} \cdot m^{-3}$], expressing flux as an area-specific vector or volume-specific vectorial or scalar quantity, respectively (Gnaiger 1993b).

We suggest to define: (*1*) *vectoral* fluxes, which are translocations as functions of *gradients* with direction in geometric space in continuous systems; (*2*) *vectorial* fluxes, which describe translocations in discontinuous systems and are restricted to information on *compartmental differences* (**Figure 3C**, transmembrane proton flux); and (*3*) *scalar* fluxes, which are transformations in a *homogenous* system (**Figure 3C**, catabolic O_2 flux, J_{kO_2}).

Vectorial transmembrane proton fluxes, J_{mH^+pos} and J_{mH^+neg}, are analyzed in a heterogenous compartmental system as a quantity with *directional* but not *spatial* information. Translocation of protons across the mtIM has a defined direction, either from the negative compartment (matrix space; negative, neg–compartment) to the positive compartment (inter-membrane space; positive, pos–compartment) or *vice versa* (**Figure 3C**). The arrows defining the direction of the translocation between the two vesicular compartments may point upwards or downwards, right or left, without any implication that these are actual directions in space. The pos–compartment is neither above nor below the neg–compartment in a spatial sense, but can be visualized arbitrarily in a figure in the upper position (**Figure 3C**). In general, the *compartmental direction* of vectorial translocation from the neg–compartment to the pos–compartment is defined by assigning the initial and final state as *ergodynamic compartments*, $H^+_{neg} \rightarrow H^+_{pos}$ or $0 = -1\ H^+_{neg} + 1\ H^+_{pos}$, related to work (erg = work) that must be performed to lift the proton from a lower to a higher electrochemical potential or from the lower to the higher ergodynamic compartment (Gnaiger 1993b).

In analogy to *vectorial* translocation, the direction of a *scalar* chemical reaction, $A \rightarrow B$ or $0 = -1\ A + 1\ B$, is defined by assigning substrates and products, A and B, as ergodynamic compartments. O_2 is defined as a substrate in respiratory O_2 consumption, which together with the fuel substrates comprises the substrate compartment of the catabolic reaction. Volume-specific scalar O_2 flux is coupled to vectorial translocation, yielding the H^+_{pos}/O_2 ratio (**Figure 2**).

3.2. Normalization for system-size: flux per chamber volume

System-specific flux, $\boldsymbol{J_{V,O_2}}$: The experimental system (experimental chamber) is part of the measurement apparatus, separated from the environment as an isolated, closed, open, isothermal or non-isothermal system (**Table 4**). On another level, we distinguish between (*1*) the *system* with volume V and mass m defined by the system boundaries, and (*2*) the *sample* or *objects* with volume V_X and mass m_X that are enclosed in the experimental chamber (**Figure 7**). Metabolic O_2 flow per object, $I_{O_2/X}$, increases as the mass of the object is increased. Sample mass-specific O_2 flux, $J_{O_2/mX}$ should be independent of the mass of the sample studied in the instrument chamber, but system volume-specific O_2 flux, J_{V,O_2} (per volume of the instrument chamber), should increase in direct proportion to the mass of the sample in the chamber. Whereas J_{V,O_2} depends on mass-concentration of the sample in the chamber, it should be independent of the chamber (system) volume at constant sample mass. There are practical limitations to increase the mass-concentration of the sample in the chamber, when one is concerned about crowding effects and instrumental time resolution.

When the reactor volume does not change during the reaction, which is typical for liquid phase reactions, the volume-specific *flux of a chemical reaction* r is the time derivative of the advancement of the reaction per unit volume, $J_{V,rB} = d_r\xi_B/dt \cdot V^{-1}$ [$(mol \cdot s^{-1}) \cdot L^{-1}$]. The *rate of concentration change* is dc_B/dt [$(mol \cdot L^{-1}) \cdot s^{-1}$], where concentration is $c_B = n_B/V$. There is a difference between (*1*) J_{V,rO_2} [$mol \cdot s^{-1} \cdot L^{-1}$] and (*2*) rate of concentration change [$mol \cdot L^{-1} \cdot s^{-1}$].

These merge to a single expression only in closed systems. In open systems, external fluxes (such as O_2 supply) are distinguished from internal transformations (catabolic flux, O_2 consumption). In a closed system, external flows of all substances are zero and O_2 consumption (internal flow of catabolic reactions k), I_{kO_2} [pmol·s^{-1}], causes a decline of the amount of O_2 in the system, n_{O_2} [nmol]. Normalization of these quantities for the volume of the system, V [L ≡ dm^3], yields volume-specific O_2 flux, $J_{V,kO_2} = I_{kO_2}/V$ [nmol·s^{-1}·L^{-1}], and O_2 concentration, [O_2] or $c_{O_2} = n_{O_2}/V$ [µmol·L^{-1} = µM = nmol·mL^{-1}]. Instrumental background O_2 flux is due to external flux into a non-ideal closed respirometer; then total volume-specific flux has to be corrected for instrumental background O_2 flux—O_2 diffusion into or out of the instrumental chamber. J_{V,kO_2} is relevant mainly for methodological reasons and should be compared with the accuracy of instrumental resolution of background-corrected flux, *e.g.*, ±1 nmol·s^{-1}·L^{-1} (Gnaiger 2001). 'Metabolic' or catabolic indicates O_2 flux, J_{kO_2}, corrected for: (*1*) instrumental background O_2 flux; (*2*) chemical background O_2 flux due to autoxidation of chemical components added to the incubation medium; and (*3*) *Rox* for O_2-consuming side reactions unrelated to the catabolic pathway k.

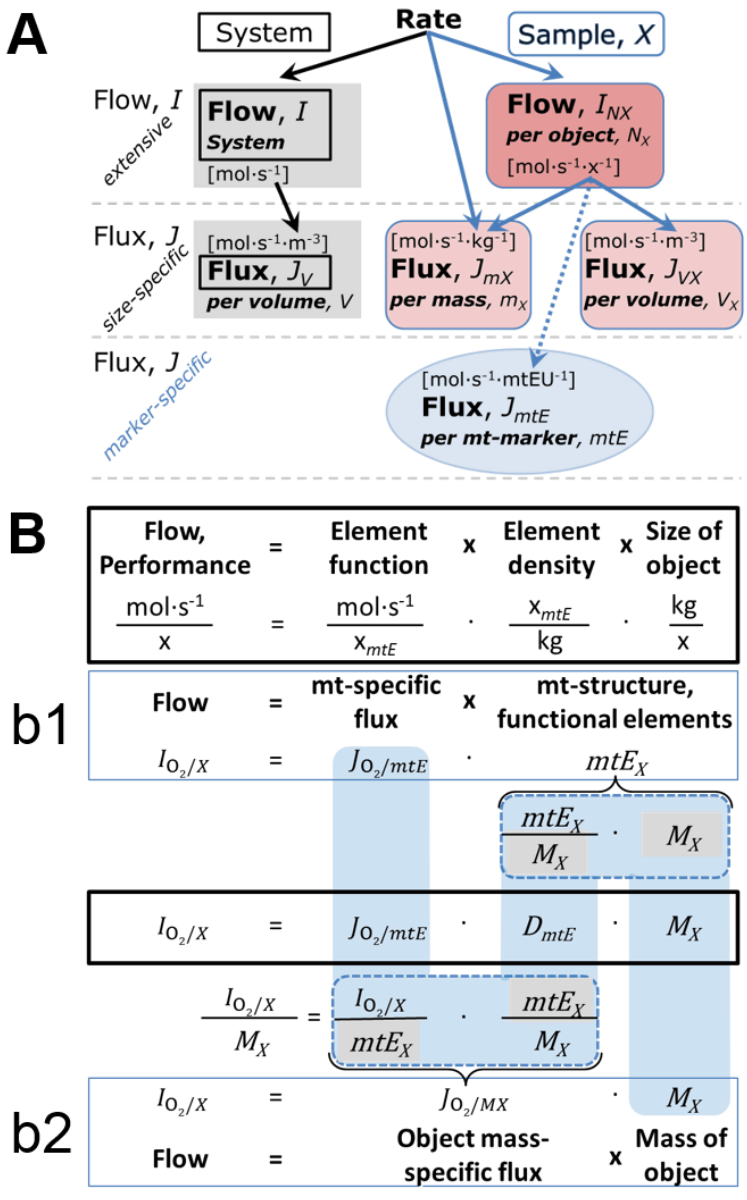

Figure 7. Flow and flux, and normalization in structure-function analysis
(**A**) Different meanings of rate may lead to confusion, if the normalization is not sufficiently specified. Results are frequently expressed as mass-specific *flux*, J_{mX}, per mg protein, dry or wet weight (mass). Cell volume, V_{cell}, may be used for normalization (volume-specific flux, J_{VCell}), which must be clearly distinguished from flow per cell, I_{Ncell}, or flux, J_V, expressed for methodological reasons per volume of the measurement system.
(**B**) O_2 flow, $I_{O_2/X}$, is the product of performance per functional element (element function, mitochondria-specific flux), element density (mitochondrial density, D_{mtE}), and size of entity X (mass, M_X). (**b1**) Structured analysis: performance is the product of mitochondrial *function* (mt-specific flux) and *structure* (functional elements; D_{mtE} times mass of X). (**b2**) Unstructured analysis: performance is the product of *entity mass-specific flux*, $J_{O_2/MX} = I_{O_2/X}/M_X = I_{O_2}/m_X$ [mol·s^{-1}·kg^{-1}] and *size of entity*, expressed as mass of X; $M_X = m_X \cdot N_X^{-1}$ [kg·x^{-1}]. Modified from Gnaiger (2014). For further details see **Table 4**.

3.3. Normalization: per sample

The challenges of measuring mitochondrial respiratory flux are matched by those of normalization. Application of common and defined units is required for direct transfer of reported results into a database. The second [s] is the *SI* unit for the base quantity *time*. It is also the standard time-unit used in solution chemical kinetics. A rate may be considered as the numerator and normalization as the complementary denominator, which are tightly linked in reporting the measurements in a format commensurate with the requirements of a database. Normalization (**Table 4**) is guided by physicochemical principles, methodological considerations, and conceptual strategies (**Figure 7**).

Table 4. Sample concentrations and normalization of flux.

Expression	Symbol	Definition	Unit	Notes
Sample				
identity of sample	X	object: cell, tissue, animal, patient		
number of sample entities X	N_X	number of objects	x	
mass of sample X	m_X		kg	1
mass of object X	M_X	$M_X = m_X \cdot N_X^{-1}$	kg·x^{-1}	1
Mitochondria				
mitochondria	mt	X = mt		
amount of mt-elements	mtE	quantity of mt-marker	mtEU	
Concentrations				
object number concentration	C_{NX}	$C_{NX} = N_X \cdot V^{-1}$	x·m^{-3}	2
sample mass concentration	C_{mX}	$C_{mX} = m_X \cdot V^{-1}$	kg·m^{-3}	
mitochondrial concentration	C_{mtE}	$C_{mtE} = mtE \cdot V^{-1}$	mtEU·m^{-3}	3
specific mitochondrial density	D_{mtE}	$D_{mtE} = mtE \cdot m_X^{-1}$	mtEU·kg^{-1}	4
mitochondrial content, mtE per object X	mtE_X	$mtE_X = mtE \cdot N_X^{-1}$	mtEU·x^{-1}	5
O_2 flow and flux				6
flow, system	I_{O_2}	internal flow	mol·s^{-1}	7
volume-specific flux	J_{V,O_2}	$J_{V,O_2} = I_{O_2} \cdot V^{-1}$	mol·s^{-1}·m^{-3}	8
flow per object X	$I_{O_2/X}$	$I_{O_2/X} = J_{V,O_2} \cdot C_{NX}^{-1}$	mol·s^{-1}·x^{-1}	9
mass-specific flux	$J_{O_2/mX}$	$J_{O_2/mX} = J_{V,O_2} \cdot C_{mX}^{-1}$	mol·s^{-1}·kg^{-1}	
mitochondria-specific flux	$J_{O_2/mtE}$	$J_{O_2/mtE} = J_{V,O_2} \cdot C_{mtE}^{-1}$	mol·s^{-1}·mtEU^{-1}	10

1 The *SI* prefix k is used for the SI base unit of mass (kg = 1,000 g). In praxis, various *SI* prefixes are used for convenience, to make numbers easily readable, *e.g.,* 1 mg tissue, cell or mitochondrial mass instead of 0.000001 kg.

2 In case sample X = cells, the object number concentration is $C_{N\mathrm{cell}} = N_{\mathrm{cell}} \cdot V^{-1}$, and volume may be expressed in [dm^3 ≡ L] or [cm^3 = mL]. See **Table 5** for different object types.

3 mt-concentration is an experimental variable, dependent on sample concentration: (*1*) $C_{mtE} = mtE \cdot V^{-1}$; (*2*) $C_{mtE} = mtE_X \cdot C_{NX}$; (*3*) $C_{mtE} = C_{mX} \cdot D_{mtE}$.

4 If the amount of mitochondria, mtE, is expressed as mitochondrial mass, then D_{mtE} is the mass fraction of mitochondria in the sample. If mtE is expressed as mitochondrial volume, V_{mt}, and the mass of sample, m_X, is replaced by volume of sample, V_X, then D_{mtE} is the volume fraction of mitochondria in the sample.

5 $mtE_X = mtE \cdot N_X^{-1} = C_{mtE} \cdot C_{NX}^{-1}$.

6 O_2 can be replaced by other chemicals B to study different reactions, *e.g.,* ATP, H_2O_2, or vesicular compartmental translocations, *e.g.,* Ca^{2+}.

7 I_{O_2} and V are defined per instrument chamber as a system of constant volume (and constant temperature), which may be closed or open. I_{O_2} is abbreviated for I_{rO_2}, *i.e.*, the metabolic or internal O_2 flow of the chemical reaction r in which O_2 is consumed, hence the negative stoichiometric number, $\nu_{O_2} = -1$. $I_{rO_2} = d_r n_{O_2}/dt \cdot \nu_{O_2}^{-1}$. If r includes all chemical reactions in which O_2 participates, then $d_r n_{O_2} = dn_{O_2} - d_e n_{O_2}$, where dn_{O_2} is the change in the amount of O_2 in the instrument chamber and $d_e n_{O_2}$ is the amount of O_2 added externally to the system. At steady state, by definition $dn_{O_2} = 0$, hence $d_r n_{O_2} = -d_e n_{O_2}$.

8 J_{V,O_2} is an experimental variable, expressed per volume of the instrument chamber.

9 $I_{O_2/X}$ is a physiological variable, depending on the size of entity X.

10 There are many ways to normalize for a mitochondrial marker, that are used in different experimental approaches: (*1*) $J_{O_2/mtE} = J_{V,O_2} \cdot C_{mtE}^{-1}$; (*2*) $J_{O_2/mtE} = J_{V,O_2} \cdot C_{mX}^{-1} \cdot D_{mtE}^{-1} = J_{O_2/mX} \cdot D_{mtE}^{-1}$; (*3*) $J_{O_2/mtE} = J_{V,O_2} \cdot C_{NX}^{-1} \cdot mtE_X^{-1} = I_{O_2/X} \cdot mtE_X^{-1}$; (*4*) $J_{O_2/mtE} = I_{O_2} \cdot mtE^{-1}$. The mt-elemental unit [mtEU] varies between different mt-markers.

Sample concentration, C_{mX}: Normalization for sample concentration is required to report respiratory data. Considering a tissue or cells as the sample, X, the sample mass is m_X [mg], which is frequently measured as wet or dry weight, W_w or W_d [mg], respectively, or as amount of tissue or cell protein, $m_{Protein}$. In the case of permeabilized tissues, cells, and homogenates, the sample concentration, $C_{mX} = m_X/V$ [$g \cdot L^{-1}$ = $mg \cdot mL^{-1}$], is the mass of the subsample of tissue that is transferred into the instrument chamber.

Mass-specific flux, $J_{O_2/mX}$: Mass-specific flux is obtained by expressing respiration per mass of sample, m_X [mg]. X is the type of sample—isolated mitochondria, tissue homogenate, permeabilized fibres or cells. Volume-specific flux is divided by mass concentration of X, $J_{O_2/mX} = J_{V,O_2}/C_{mX}$; or flow per cell is divided by mass per cell, $J_{O_2/mcell} = I_{O_2/cell}/M_{cell}$. If mass-specific O_2 flux is constant and independent of sample size (expressed as mass), then there is no interaction between the subsystems. A 1.5 mg and a 3.0 mg muscle sample respires at identical mass-specific flux. Mass-specific O_2 flux, however, may change with the mass of a tissue sample, cells or isolated mitochondria in the measuring chamber, in which the nature of the interaction becomes an issue. Therefore, cell density must be optimized, particularly in experiments carried out in wells, considering the confluency of the cell monolayer or clumps of cells (Salabei *et al.* 2014).

Number concentration, C_{NX}: C_{NX} is the experimental *number concentration* of sample X. In the case of cells or animals, *e.g.*, nematodes, $C_{NX} = N_X/V$ [$x \cdot L^{-1}$], where N_X is the number of cells or organisms in the chamber (**Table 4**).

Flow per object, $I_{O_2/X}$: A special case of normalization is encountered in respiratory studies with permeabilized (or intact) cells. If respiration is expressed per cell, the O_2 flow per measurement system is replaced by the O_2 flow per cell, $I_{O_2/cell}$ (**Table 4**). O_2 flow can be calculated from volume-specific O_2 flux, J_{V,O_2} [$nmol \cdot s^{-1} \cdot L^{-1}$] (per V of the measurement chamber [L]), divided by the number concentration of cells, $C_{Ncell} = N_{cell}/V$ [$cell \cdot L^{-1}$], where N_{cell} is the number of cells in the chamber. The total cell count is the sum of viable and dead cells, $N_{cell} = N_{vce} + N_{dce}$ (**Table 5**). The cell viability index, $CVI = N_{vce}/N_{cell}$, is the ratio of viable cells (N_{vce}; before experimental permeabilization) per total cell count. After experimental permeabilization, all cells are permeabilized, $N_{pce} = N_{cell}$. The cell viability index can be used to normalize respiration for the number of cells that have been viable before experimental permeabilization, $I_{O_2/vce} = I_{O_2/cell}/CVI$, considering that mitochondrial respiratory dysfunction in dead cells should be eliminated as a confounding factor.

Cellular O_2 flow can be compared between cells of identical size. To take into account changes and differences in cell size, normalization is required to obtain cell size-specific or mitochondrial marker-specific O_2 flux (Renner *et al.* 2003).

The complexity changes when the sample is a whole organism studied as an experimental model. The scaling law in respiratory physiology reveals a strong interaction of O_2 flow and individual body mass of an organism, since *basal* metabolic rate (flow) does not increase linearly with body mass, whereas *maximum* mass-specific O_2 flux, $\dot{V}_{O2max}$ or $\dot{V}_{O2peak}$, is

approximately constant across a large range of individual body mass (Weibel and Hoppeler 2005), with individuals, breeds, and species deviating substantially from this relationship. $\dot{V}_{O2peak}$ of human endurance athletes is 60 to 80 mL $O_2 \cdot min^{-1} \cdot kg^{-1}$ body mass, converted to $J_{O_2peak/M}$ of 45 to 60 $nmol \cdot s^{-1} \cdot g^{-1}$ (Gnaiger 2014; **Table 6**).

Table 5. Sample types, *X*, abbreviations, and quantification.

Identity of sample	X	N_X	**Mass**[a]	**Volume**	**mt-Marker**
mitochondrial preparation	mt-prep	[x]	[kg]	[m^3]	[mtEU]
isolated mitochondria	imt		m_{mt}	V_{mt}	mtE
tissue homogenate	thom		m_{thom}		mtE_{thom}
permeabilized tissue	pti		m_{pti}		mtE_{pti}
permeabilized fibre	pfi		m_{pfi}		mtE_{pfi}
permeabilized cell	pce	N_{pce}	M_{pce}	V_{pce}	mtE_{pce}
cells[b]	cell	N_{cell}	M_{cell}	V_{cell}	mtE_{cell}
intact cell, viable cell	vce	N_{vce}	M_{vce}	V_{vce}	
dead cell	dce	N_{dce}	M_{dce}	V_{dce}	
organism	org	N_{org}	M_{org}	V_{org}	

[a] Instead of mass, the wet weight or dry weight is frequently stated, W_w or W_d. m_X is mass of the sample [kg], M_X is mass of the object [$kg \cdot x^{-1}$].

[b] Total cell count, $N_{cell} = N_{vce} + N_{dce}$

3.4. Normalization for mitochondrial content

Tissues can contain multiple cell populations that may have distinct mitochondrial subtypes. Mitochondria undergo dynamic fission and fusion cycles, and can exist in multiple stages and sizes that may be altered by a range of factors. The isolation of mitochondria (often achieved through differential centrifugation) can therefore yield a subsample of the mitochondrial types present in a tissue, depending on the isolation protocols utilized (*e.g.*, centrifugation speed). This possible bias should be taken into account when planning experiments using isolated mitochondria. Different sizes of mitochondria are enriched at specific centrifugation speeds, which can be used strategically for isolation of mitochondrial subpopulations.

Part of the mitochondrial content of a tissue is lost during preparation of isolated mitochondria. The fraction of isolated mitochondria obtained from a tissue sample is expressed as mitochondrial recovery. At a high mitochondrial recovery the fraction of isolated mitochondria is more representative of the total mitochondrial population than in preparations characterized by low recovery. Determination of the mitochondrial recovery and yield is based on measurement of the concentration of a mitochondrial marker in the stock of isolated mitochondria, $C_{mtE,stock}$, and crude tissue homogenate, $C_{mtE,thom}$, which simultaneously provides information on the specific mitochondrial density in the sample, D_{mtE} (**Table 4**).

Normalization is a problematic subject; it is essential to consider the question of the study. If the study aims at comparing tissue performance—such as the effects of a treatment on a specific tissue, then normalization for tissue mass or protein content is appropriate. However, if the aim is to find differences on mitochondrial function independent of mitochondrial density (**Table 4**), then normalization to a mitochondrial marker is imperative (**Figure 7**). One cannot assume that quantitative changes in various markers—such as mitochondrial proteins—necessarily occur in parallel with one another. It should be established that the marker chosen is not selectively altered by the performed treatment. In conclusion, the normalization must reflect the question under investigation to reach a satisfying answer. On the other hand, the goal of comparing results across projects and institutions requires standardization on normalization for entry into a databank.

Mitochondrial concentration, C_{mtE}, and mitochondrial markers: Mitochondrial organelles comprise a dynamic cellular reticulum in various states of fusion and fission. Hence, the definition of an "amount" of mitochondria is often misconceived: mitochondria cannot be counted reliably as a number of occurring elements. Therefore, quantification of the "amount" of mitochondria depends on the measurement of chosen mitochondrial markers. 'Mitochondria are the structural and functional elemental units of cell respiration' (Gnaiger 2014). The quantity of a mitochondrial marker can reflect the amount of *mitochondrial elements*, *mtE*, expressed in various mitochondrial elemental units [mtEU] specific for each measured mt-marker (**Table 4**). However, since mitochondrial quality may change in response to stimuli—particularly in mitochondrial dysfunction and after exercise training (Pesta *et al.* 2011; Campos *et al.* 2017)—some markers can vary while others are unchanged: (*1*) Mitochondrial volume and membrane area are structural markers, whereas mitochondrial protein mass is frequently used as a marker for isolated mitochondria. (*2*) Molecular and enzymatic mitochondrial markers (amounts or activities) can be selected as matrix markers, *e.g.*, citrate synthase activity, mtDNA; mtIM-markers, *e.g.*, cytochrome *c* oxidase activity, aa_3 content, cardiolipin, or mtOM-markers, *e.g.*, TOM20. (*3*) Extending the measurement of mitochondrial marker enzyme activity to mitochondrial pathway capacity, ET- or OXPHOS-capacity can be considered as an integrative functional mitochondrial marker.

Depending on the type of mitochondrial marker, the mitochondrial elements, *mtE*, are expressed in marker-specific units. Mitochondrial concentration in the measurement chamber and the tissue of origin are quantified as (*1*) a quantity for normalization in functional analyses, C_{mtE}, and (*2*) a physiological output that is the result of mitochondrial biogenesis and degradation, D_{mtE}, respectively (**Table 4**). It is recommended, therefore, to distinguish *experimental mitochondrial concentration*, $C_{mtE} = mtE/V$ and *physiological mitochondrial density*, $D_{mtE} = mtE/m_X$. Then mitochondrial density is the amount of mitochondrial elements per mass of tissue, which is a biological variable (**Figure 7**). The experimental variable is mitochondrial density multiplied by sample mass concentration in the measuring chamber, $C_{mtE} = D_{mtE} \cdot C_{mX}$, or mitochondrial content multiplied by sample number concentration, $C_{mtE} = mtE_X \cdot C_{NX}$ (**Table 4**).

Mitochondria-specific flux, $J_{O_2/mtE}$: Volume-specific metabolic O_2 flux depends on: (*1*) the sample concentration in the volume of the instrument chamber, C_{mX}, or C_{NX}; (*2*) the mitochondrial density in the sample, $D_{mtE} = mtE/m_X$ or $mtE_X = mtE/N_X$; and (*3*) the specific mitochondrial activity or performance per elemental mitochondrial unit, $J_{O_2/mtE} = J_{V,O_2}/C_{mtE}$ [mol·s^{-1}·mtEU^{-1}] (**Table 4**). Obviously, the numerical results for $J_{O_2/mtE}$ vary with the type of mitochondrial marker chosen for measurement of *mtE* and $C_{mtE} = mtE/V$ [mtEU·m^{-3}].

3.5. Evaluation of mitochondrial markers

Different methods are implicated in the quantification of mitochondrial markers and have different strengths. Some problems are common for all mitochondrial markers, *mtE*: (*1*) Accuracy of measurement is crucial, since even a highly accurate and reproducible measurement of O_2 flux results in an inaccurate and noisy expression if normalized by a biased and noisy measurement of a mitochondrial marker. This problem is acute in mitochondrial respiration because the denominators used (the mitochondrial markers) are often small moieties of which accurate and precise determination is difficult. This problem can be avoided when O_2 fluxes measured in substrate-uncoupler-inhibitor titration protocols are normalized for flux in a defined respiratory reference state, which is used as an *internal* marker and yields flux control ratios, *FCR*s. *FCR*s are independent of *externally* measured markers and, therefore, are statistically robust, considering the limitations of ratios in general (Jasienski and Bazzaz 1999). *FCR*s indicate qualitative changes of mitochondrial respiratory control, with highest quantitative resolution, separating the effect of mitochondrial density or concentration on $J_{O_2/mX}$

and $I_{O_2/X}$ from that of function per elemental mitochondrial marker, $J_{O_2/mtE}$ (Pesta *et al.* 2011; Gnaiger 2014). (*2*) If mitochondrial quality does not change and only the amount of mitochondria varies as a determinant of mass-specific flux, any marker is equally qualified in principle; then in practice selection of the optimum marker depends only on the accuracy and precision of measurement of the mitochondrial marker. (*3*) If mitochondrial flux control ratios change, then there may not be any best mitochondrial marker. In general, measurement of multiple mitochondrial markers enables a comparison and evaluation of normalization for a variety of mitochondrial markers. Particularly during postnatal development, the activity of marker enzymes—such as cytochrome *c* oxidase and citrate synthase—follows different time courses (Drahota *et al.* 2004). Evaluation of mitochondrial markers in healthy controls is insufficient for providing guidelines for application in the diagnosis of pathological states and specific treatments.

In line with the concept of the respiratory control ratio (Chance and Williams 1955a), the most readily used normalization is that of flux control ratios and flux control factors (Gnaiger 2014). Selection of the state of maximum flux in a protocol as the reference state has the advantages of: (*1*) internal normalization; (*2*) statistical linearization of the response in the range of 0 to 1; and (*3*) consideration of maximum flux for integrating a large number of elemental steps in the OXPHOS- or ET-pathways. This reduces the risk of selecting a functional marker that is specifically altered by the treatment or pathology, yet increases the chance that the highly integrative pathway is disproportionately affected, *e.g.*, the OXPHOS- rather than ET-pathway in case of an enzymatic defect in the phosphorylation-pathway. In this case, additional information can be obtained by reporting flux control ratios based on a reference state which indicates stable tissue-mass specific flux. Stereological determination of mitochondrial content via two-dimensional transmission electron microscopy can have limitations due to the dynamics of mitochondrial size (Meinild Lundby *et al.* 2017). Accurate determination of three-dimensional volume by two-dimensional microscopy can be both time consuming and statistically challenging (Larsen *et al.* 2012).

The validity of using mitochondrial marker enzymes (citrate synthase activity, Complex I–IV amount or activity) for normalization of flux is limited in part by the same factors that apply to flux control ratios. Strong correlations between various mitochondrial markers and citrate synthase activity (Reichmann *et al.* 1985; Boushel *et al.* 2007; Mogensen *et al.* 2007) are expected in a specific tissue of healthy subjects and in disease states not specifically targeting citrate synthase. Citrate synthase activity is acutely modifiable by exercise (Tonkonogi *et al.* 1997; Leek *et al.* 2001). Evaluation of mitochondrial markers related to a selected age and sex cohort cannot be extrapolated to provide recommendations for normalization in respirometric diagnosis of disease, in different states of development and ageing, different cell types, tissues, and species. mtDNA normalized to nDNA via qPCR is correlated to functional mitochondrial markers including OXPHOS- and ET-capacity in some cases (Puntschart *et al.* 1995; Wang *et al.* 1999; Menshikova *et al.* 2006; Boushel *et al.* 2007), but lack of such correlations have been reported (Menshikova *et al.* 2005; Schultz and Wiesner 2000; Pesta *et al.* 2011). Several studies indicate a strong correlation between cardiolipin content and increase in mitochondrial function with exercise (Menshikova *et al.* 2005; Menshikova *et al.* 2007; Larsen *et al.* 2012; Faber *et al.* 2014), but it has not been evaluated as a general mitochondrial biomarker in disease.

3.6. Conversion: units

Many different units have been used to report the O_2 consumption rate, OCR (**Table 6**). *SI* base units provide the common reference to introduce the theoretical principles (**Figure 7**), and are used with appropriately chosen *SI* prefixes to express numerical data in the most practical format, with an effort towards unification within specific areas of application (**Table**

7). Reporting data in *SI* units—including the mole [mol], coulomb [C], joule [J], and second [s]—should be encouraged, particularly by journals which propose the use of *SI* units.

Although volume is expressed as m^3 using the *SI* base unit, the litre [dm^3] is a conventional unit of volume for concentration and is used for most solution chemical kinetics. If one multiplies $I_{O_2/cell}$ by C_{Ncell}, then the result will not only be the amount of O_2 [mol] consumed per time [s^{-1}] in one litre [L^{-1}], but also the change in O_2 concentration per second (for any volume of an ideally closed system). This is ideal for kinetic modeling as it blends with chemical rate equations where concentrations are typically expressed in $mol \cdot L^{-1}$ (Wagner *et al.* 2011). In studies of multinuclear cells—such as differentiated skeletal muscle cells—it is easy to determine the number of nuclei but not the total number of cells. A generalized concept, therefore, is obtained by substituting cells by nuclei as the sample entity. This does not hold, however, for enucleated platelets.

Table 6. Conversion of various units used in respirometry and ergometry. e^- is the number of electrons or reducing equivalents. z_B is the charge number of entity B.

1 Unit		x	Multiplication factor	*SI*-unit	Note
ng.atom $O \cdot s^{-1}$	(2 e^-)		0.5	nmol $O_2 \cdot s^{-1}$	
ng.atom $O \cdot min^{-1}$	(2 e^-)		8.33	pmol $O_2 \cdot s^{-1}$	
natom $O \cdot min^{-1}$	(2 e^-)		8.33	pmol $O_2 \cdot s^{-1}$	
nmol $O_2 \cdot min^{-1}$	(4 e^-)		16.67	pmol $O_2 \cdot s^{-1}$	
nmol $O_2 \cdot h^{-1}$	(4 e^-)		0.2778	pmol $O_2 \cdot s^{-1}$	
mL $O_2 \cdot min^{-1}$ at STPD[a]			0.744	µmol $O_2 \cdot s^{-1}$	1
W = J/s at -470 kJ/mol O_2			-2.128	µmol $O_2 \cdot s^{-1}$	
mA = mC·s^{-1}	(z_{H^+} = 1)		10.36	nmol $H^+ \cdot s^{-1}$	2
mA = mC·s^{-1}	(z_{O_2} = 4)		2.59	nmol $O_2 \cdot s^{-1}$	2
nmol $H^+ \cdot s^{-1}$	(z_{H^+} = 1)		0.09649	mA	3
nmol $O_2 \cdot s^{-1}$	(z_{O_2} = 4)		0.38594	mA	3

1 At standard temperature and pressure dry (STPD: 0 °C = 273.15 K and 1 atm = 101.325 kPa = 760 mmHg), the molar volume of an ideal gas, V_m, and V_{m,O_2} is 22.414 and 22.392 $L \cdot mol^{-1}$, respectively. Rounded to three decimal places, both values yield the conversion factor of 0.744. For comparison at normal temperature and pressure dry (NTPD: 20 °C), V_{m,O_2} is 24.038 $L \cdot mol^{-1}$. Note that the *SI* standard pressure is 100 kPa.

2 The multiplication factor is $10^6/(z_B \cdot F)$.

3 The multiplication factor is $z_B \cdot F/10^6$.

For studies of cells, we recommend that respiration be expressed, as far as possible, as: (*1*) O_2 flux normalized for a mitochondrial marker, for separation of the effects of mitochondrial quality and content on cell respiration (this includes *FCR*s as a normalization for a functional mitochondrial marker); (*2*) O_2 flux in units of cell volume or mass, for comparison of respiration of cells with different cell size (Renner *et al.* 2003) and with studies on tissue preparations, and (*3*) O_2 flow in units of attomole (10^{-18} mol) of O_2 consumed in a second by each cell [$amol \cdot s^{-1} \cdot cell^{-1}$], numerically equivalent to [$pmol \cdot s^{-1} \cdot 10^{-6}$ cells]. This convention allows information to be easily used when designing experiments in which O_2 flow must be considered. For example, to estimate the volume-specific O_2 flux in an instrument chamber that would be expected at a particular cell number concentration, one simply needs to multiply the flow per cell by the number of cells per volume of interest. This provides the amount of O_2 [mol]

consumed per time [s^{-1}] per unit volume [L^{-1}]. At an O_2 flow of 100 amol·s^{-1}·$cell^{-1}$ and a cell density of 10^9 cells·L^{-1} (10^6 cells·mL^{-1}), the volume-specific O_2 flux is 100 nmol·s^{-1}·L^{-1} (100 pmol·s^{-1}·mL^{-1}).

Table 7. Conversion of units with preservation of numerical values.

Name	Frequently used unit	Equivalent unit	Note
volume-specific flux, J_{V,O_2}	pmol·s^{-1}·mL^{-1}	nmol·s^{-1}·L^{-1}	1
	mmol·s^{-1}·L^{-1}	mol·s^{-1}·m^{-3}	
cell-specific flow, $I_{O_2/cell}$	pmol·s^{-1}·10^{-6} cells	amol·s^{-1}·$cell^{-1}$	2
	pmol·s^{-1}·10^{-9} cells	zmol·s^{-1}·$cell^{-1}$	3
cell number concentration, C_{Nce}	10^6 cells·mL^{-1}	10^9 cells·L^{-1}	
mitochondrial protein concentration, C_{mtE}	0.1 mg·mL^{-1}	0.1 g·L^{-1}	
mass-specific flux, $J_{O_2/m}$	pmol·s^{-1}·mg^{-1}	nmol·s^{-1}·g^{-1}	4
catabolic power, P_k	µW·10^{-6} cells	pW·$cell^{-1}$	1
volume	1,000 L	m^3 (1,000 kg)	
	L	dm^3 (kg)	
	mL	cm^3 (g)	
	µL	mm^3 (mg)	
	fL	$µm^3$ (pg)	5
amount of substance concentration	M = mol·L^{-1}	mol·dm^{-3}	

1 pmol: picomole = 10^{-12} mol
2 amol: attomole = 10^{-18} mol
3 zmol: zeptomole = 10^{-21} mol
4 nmol: nanomole = 10^{-9} mol
5 fL: femtolitre = 10^{-15} L

ET-capacity in human cell types including HEK 293, primary HUVEC and fibroblasts ranges from 50 to 180 amol·s^{-1}·$cell^{-1}$, measured in intact cells in the noncoupled state (see Gnaiger 2014). At 100 amol·s^{-1}·$cell^{-1}$ corrected for *Rox*, the current across the mt-membranes, I_{H^+e}, approximates 193 pA·$cell^{-1}$ or 0.2 nA per cell. See Rich (2003) for an extension of quantitative bioenergetics from the molecular to the human scale, with a transmembrane proton flux equivalent to 520 A in an adult at a catabolic power of -110 W. Modelling approaches illustrate the link between protonmotive force and currents (Willis *et al.* 2016).

We consider isolated mitochondria as powerhouses and proton pumps as molecular machines to relate experimental results to energy metabolism of the intact cell. The cellular P»/O_2 based on oxidation of glycogen is increased by the glycolytic (fermentative) substrate-level phosphorylation of 3 P»/Glyc or 0.5 mol P» for each mol O_2 consumed in the complete oxidation of a mol glycosyl unit (Glyc). Adding 0.5 to the mitochondrial P»/O_2 ratio of 5.4 yields a bioenergetic cell physiological P»/O_2 ratio close to 6. Two NADH equivalents are formed during glycolysis and transported from the cytosol into the mitochondrial matrix, either by the malate-aspartate shuttle or by the glycerophosphate shuttle (**Figure 2**) resulting in different theoretical yields of ATP generated by mitochondria, the energetic cost of which potentially must be taken into account. Considering also substrate-level phosphorylation in the TCA cycle, this high P»/O_2 ratio not only reflects proton translocation and OXPHOS studied in isolation, but integrates mitochondrial physiology with energy transformation in the living cell (Gnaiger 1993a).

4. Conclusions

MitoEAGLE can serve as a gateway to better diagnose mitochondrial respiratory defects linked to genetic variation, age-related health risks, sex-specific mitochondrial performance, lifestyle with its effects on degenerative diseases, and thermal and chemical environment. The present recommendations on coupling control states and rates, linked to the concept of the protonmotive force, are focused on studies with mitochondrial preparations. These will be extended in a series of reports on pathway control of mitochondrial respiration, respiratory states in intact cells, and harmonization of experimental procedures.

OXPHOS analysis is based on the study of mitochondrial preparations complementary to bioenergetic investigations of intact cells and organisms—from animal models to healthy persons or patients. Metabolic fluxes measured in defined coupling and pathway control states provide insights into the meaning of cellular and organismic respiration. An O_2 flux balance scheme illustrates the relationships and general definitions (**Figures 1 and 2**).

Catabolic cell respiration is the process of exergonic and exothermic energy transformation in which scalar redox reactions are coupled to vectorial ion translocation across a semipermeable membrane, which separates the small volume of a bacterial cell or mitochondrion from the larger volume of its surroundings. The electrochemical exergy can be partially conserved in the phosphorylation of ADP to ATP or in ion pumping, or dissipated in an electrochemical short-circuit. Respiration is thus clearly distinguished from fermentation as the counterpart of cellular core energy metabolism. Respiration is separated in mitochondrial preparations from the interactions with the fermentative pathways of the intact cell.

The optimal choice for expressing mitochondrial and cell respiration as O_2 flow per biological sample, and normalization for specific tissue-markers (volume, mass, protein) and mitochondrial markers (volume, protein, content, mtDNA, activity of marker enzymes, respiratory reference state) is guided by the scientific question under study. Interpretation of the data depends critically on appropriate normalization.

We recommend for studies with mitochondrial preparations:

- Normalization of respiratory rates should be provided as far as possible:
    1. Biophysical normalization: on a per cell basis as O_2 flow; this may not be possible when dealing with tissues
    2. Cellular normalization: per g cell or tissue protein, or per cell or tissue mass as mass-specific O_2 flux
    3. Mitochondrial normalization: per mitochondrial marker as mt-specific flux.

  With information on cell size and the use of multiple normalizations, maximum potential information is available (Renner *et al.* 2003; Wagner *et al.* 2011; Gnaiger 2014). Reporting flow in a respiratory chamber [nmol·s^{-1}] is discouraged, since it restricts the analysis to intra-experimental comparison of relative (qualitative) differences.
- Catabolic mitochondrial respiration is distinguished from residual oxygen consumption. Fluxes in mitochondrial coupling states should be, as far as possible, corrected for residual oxygen consumption.
- Different mechanisms of uncoupling should be distinguished by defined terms. The tightness of coupling relates to these uncoupling mechanisms, whereas the coupling stoichiometry varies as a function the substrate type undergoing oxidation in ET-pathways with either three or two redox proton pumps operating in series. Separation of tightness of coupling from coupling stoichiometry is possible only in well defined ET-pathway control states with simple substrate-inhibitor combinations.
- In studies of isolated mitochondria, the mitochondrial recovery and yield should be reported. Experimental criteria for evaluation of purity versus integrity should be considered. Mitochondrial markers—such as citrate synthase activity as an enzymatic matrix marker—provide a link to the tissue of origin on the basis of calculating the

mitochondrial recovery, *i.e.*, the fraction of mitochondrial marker obtained from a unit mass of tissue. Total mitochondrial protein is frequently applied as a mitochondrial marker, which is restricted to isolated mitochondria.

- In studies of permeabilized cells, the viability of the cell culture or cell suspension of origin should be reported. Normalization should be evaluated for total cell count or viable cell count.
- Terms and symbols are summarized in **Table 8**. Their use will facilitate transdisciplinary communication and support further developments towards a consistent theory of bioenergetics and mitochondrial physiology. Technical terms related to and defined with normal words can be used as index terms in databases, support the creation of ontologies towards semantic information processing (MitoPedia), and help in communicating analytical findings as impactful data-driven stories. '*Making data available without making it understandable may be worse than not making it available at all*' (National Academies of Sciences, Engineering, and Medicine 2018). Success will depend on taking next steps: (*1*) exhaustive text-mining considering Omics data and functional data; (*2*) network analysis of Omics data with bioinformatics tools; (*3*) cross-validation with distinct bioinformatics approaches; (*4*) correlation with functional data; (*5*) guidelines for biological validation of network data. This is a call to carefully contribute to FAIR principles (Findable, Accessible, Interoperable, Reusable) for the sharing of scientific data.

Table 8. Terms, symbols, and units.

Term	Symbol	Unit	Links and comments
alternative quinol oxidase	AOX		Figure 3A
amount of substance B	n_B	[mol]	
ATP yield per O_2	$Y_{P»/O2}$		P»/O2 ratio measured in any respiratory state
catabolic reaction	k		Figure 1 and 3
catabolic respiration	J_{kO2}	*varies*	Figure 1 and 3
cell number	N_{cell}	[x]	Table 5; $N_{cell} = N_{vce} + N_{dce}$
cell respiration	J_{rO2}	*varies*	Figure 1
cell viability index	*CVI*		$CVI = N_{vce}/N_{cell} = 1- N_{dce}/N_{cell}$
Complexes I to IV	CI to CIV		respiratory ET Complexes; Figure 3A
concentration of substance B	$c_B = n_B \cdot V^{-1}$; [B]	[mol·m^{-3}]	Box 2
dead cell number	N_{dce}	[x]	Table 5; non-viable cells, loss of plasma membrane barrier function
electron transfer system	ETS		Figure 3A, Figure 5; state
flow, for substance B	I_B	[mol·s^{-1}]	system-related extensive quantity; Figure 7
flux, for substance B	J_B	*varies*	size-specific quantitiy; Figure 7
inorganic phosphate	P_i		Figure 3C
intact cell number, viable cell number	N_{vce}	[x]	Table 5; viable cells, intact of plasma membrane barrier function
LEAK	LEAK		Table 1, Figure 5; state
mass of sample *X*	m_X	[kg]	Table 4
mass of entity *X*	M_X	[kg]	mass of object *X*; Table 4
MITOCARTA			https://www.broadinstitute.org/scientific-community/science/programs/metabolic-disease-program/publications/mitocarta/mitocarta-in-0
MitoPedia			http://www.bioblast.at/index.php/MitoPedia
mitochondria or mitochondrial	mt		Box 1

mitochondrial DNA	mtDNA		Box 1
mitochondrial concentration	$C_{mtE} = mtE \cdot V^{-1}$	[mtEU·m^{-3}]	Table 4
mitochondrial content	$mtE_X = mtE \cdot N_X^{-1}$	[mtEU·x^{-1}]	Table 4
mitochondrial elemental unit	mtEU	*varies*	Table 4, specific units for mt-marker
mitochondrial inner membrane	mtIM		Figure 2; MIM is widely used; the first M is replaced by mt; Box 1
mitochondrial outer membrane	mtOM		Figure 2; MOM is widely used; the first M is replaced by mt; Box 1
mitochondrial recovery	Y_{mtE}		fraction of *mtE* recovered in sample from the tissue of origin
mitochondrial yield	$Y_{mtE/m}$		$Y_{mtE/m} = Y_{mtE} \cdot D_{mtE}$
negative	neg		Figure 3C
number concentration of *X*	C_{NX}	[x·m^{-3}]	Table 4
number of entities *X*	N_X	[x]	Table 4, Figure 7
number of entity B	N_B	[x]	Table 4
oxidative phosphorylation	OXPHOS		Table 1, Figure 5; state
oxygen concentration	$c_{O2} = n_{O2} \cdot V^{-1}$; [$O_2$]	[mol·m^{-3}]	Section 3.2
oxygen flux, in reaction r	J_{rO2}	*varies*	Figure 1
permeabilized cell number	N_{pce}	[x]	Table 5; experimental permeabilization of plasma membrane; $N_{pce} = N_{cell}$
phosphorylation of ADP to ATP	P»		Section 2.2
positive	pos		Figure 3C
proton in the negative compartment	H^+_{neg}		Figure 3C
proton in the positive compartment	H^+_{pos}		Figure 3C
rate of electron transfer in ET state	*E*		ET-capacity; Table 1
rate of LEAK respiration	*L*		Table 1
rate of oxidative phosphorylation	*P*		OXPHOS capacity; Table 1
rate of residual oxygen consumption	*Rox*		Table 1, Figure 1
residual oxygen consumption	ROX		Table 1; state
respiratory supercomplex	SC $I_nIII_nIV_n$		Box 1; supramolecular assemblies composed of variable copy numbers (*n*) of CI, CIII and CIV
specific mitochondrial density	$D_{mtE} = mtE \cdot m_X^{-1}$	[mtEU·kg^{-1}]	Table 4
volume	*V*	[m^{-3}]	Table 7
weight, dry weight	W_d	[kg]	used as mass of sample *X*; Figure 7
weight, wet weight	W_w	[kg]	used as mass of sample *X*; Figure 7

Acknowledgements

We thank M. Beno for management assistance. Supported by COST Action CA15203 MitoEAGLE and K-Regio project MitoFit (E.G.).

Competing financial interests: E.G. is founder and CEO of Oroboros Instruments, Innsbruck, Austria.

5. References

Altmann R (1894) Die Elementarorganismen und ihre Beziehungen zu den Zellen. Zweite vermehrte Auflage. Verlag Von Veit & Comp, Leipzig:160 pp.

Beard DA (2005) A biophysical model of the mitochondrial respiratory system and oxidative phosphorylation. PLoS Comput Biol 1(4):e36.

Benda C (1898) Weitere Mitteilungen über die Mitochondria. Verh Dtsch Physiol Ges:376-83.

Birkedal R, Laasmaa M, Vendelin M (2014) The location of energetic compartments affects energetic communication in cardiomyocytes. Front Physiol 5:376.

Breton S, Beaupré HD, Stewart DT, Hoeh WR, Blier PU (2007) The unusual system of doubly uniparental inheritance of mtDNA: isn't one enough? Trends Genet 23:465-74.

1499 Brown GC (1992) Control of respiration and ATP synthesis in mammalian mitochondria and cells. Biochem J
1500 284:1-13.
1501 Calvo SE, Klauser CR, Mootha VK (2016) MitoCarta2.0: an updated inventory of mammalian mitochondrial
1502 proteins. Nucleic Acids Research 44:D1251-7.
1503 Calvo SE, Julien O, Clauser KR, Shen H, Kamer KJ, Wells JA, Mootha VK (2017) Comparative analysis of
1504 mitochondrial N-termini from mouse, human, and yeast. Mol Cell Proteomics 16:512-23.
1505 Campos JC, Queliconi BB, Bozi LHM, Bechara LRG, Dourado PMM, Andres AM, Jannig PR, Gomes KMS,
1506 Zambelli VO, Rocha-Resende C, Guatimosim S, Brum PC, Mochly-Rosen D, Gottlieb RA, Kowaltowski AJ,
1507 Ferreira JCB (2017) Exercise reestablishes autophagic flux and mitochondrial quality control in heart failure.
1508 Autophagy 13:1304-317.
1509 Canton M, Luvisetto S, Schmehl I, Azzone GF (1995) The nature of mitochondrial respiration and
1510 discrimination between membrane and pump properties. Biochem J 310:477-81.
1511 Chance B, Williams GR (1955a) Respiratory enzymes in oxidative phosphorylation. I. Kinetics of oxygen
1512 utilization. J Biol Chem 217:383-93.
1513 Chance B, Williams GR (1955b) Respiratory enzymes in oxidative phosphorylation: III. The steady state. J Biol
1514 Chem 217:409-27.
1515 Chance B, Williams GR (1955c) Respiratory enzymes in oxidative phosphorylation. IV. The respiratory chain. J
1516 Biol Chem 217:429-38.
1517 Chance B, Williams GR (1956) The respiratory chain and oxidative phosphorylation. Adv Enzymol Relat Subj
1518 Biochem 17:65-134.
1519 Cobb LJ, Lee C, Xiao J, Yen K, Wong RG, Nakamura HK, Mehta HH, Gao Q, Ashur C, Huffman DM, Wan J,
1520 Muzumdar R, Barzilai N, Cohen P (2016) Naturally occurring mitochondrial-derived peptides are age-
1521 dependent regulators of apoptosis, insulin sensitivity, and inflammatory markers. Aging (Albany NY) 8:796-
1522 809.
1523 Cohen ER, Cvitas T, Frey JG, Holmström B, Kuchitsu K, Marquardt R, Mills I, Pavese F, Quack M, Stohner J,
1524 Strauss HL, Takami M, Thor HL (2008) Quantities, units and smbols in physical chemistry, IUPAC Green
1525 Book, 3rd Edition, 2nd Printing, IUPAC & RSC Publishing, Cambridge.
1526 Cooper H, Hedges LV, Valentine JC, eds (2009) The handbook of research synthesis and meta-analysis. Russell
1527 Sage Foundation.
1528 Coopersmith J (2010) Energy, the subtle concept. The discovery of Feynman's blocks from Leibnitz to Einstein.
1529 Oxford University Press:400 pp.
1530 Cummins J (1998) Mitochondrial DNA in mammalian reproduction. Rev Reprod 3:172-82.
1531 Dai Q, Shah AA, Garde RV, Yonish BA, Zhang L, Medvitz NA, Miller SE, Hansen EL, Dunn CN, Price TM
1532 (2013) A truncated progesterone receptor (PR-M) localizes to the mitochondrion and controls cellular
1533 respiration. Mol Endocrinol 27:741-53.
1534 Divakaruni AS, Brand MD (2011) The regulation and physiology of mitochondrial proton leak. Physiology
1535 (Bethesda) 26:192-205.
1536 Doerrier C, Garcia-Souza LF, Krumschnabel G, Wohlfarter Y, Mészáros AT, Gnaiger E (2018) High-Resolution
1537 FluoRespirometry and OXPHOS protocols for human cells, permeabilized fibres from small biopsies of
1538 muscle and isolated mitochondria. Methods Mol. Biol. (in press)
1539 Doskey CM, van 't Erve TJ, Wagner BA, Buettner GR (2015) Moles of a substance per cell is a highly
1540 informative dosing metric in cell culture. PLOS ONE 10:e0132572.
1541 Drahota Z, Milerová M, Stieglerová A, Houstek J, Ostádal B (2004) Developmental changes of cytochrome *c*
1542 oxidase and citrate synthase in rat heart homogenate. Physiol Res 53:119-22.
1543 Duarte FV, Palmeira CM, Rolo AP (2014) The role of microRNAs in mitochondria: small players acting wide.
1544 Genes (Basel) 5:865-86.
1545 Ernster L, Schatz G (1981) Mitochondria: a historical review. J Cell Biol 91:227s-55s.
1546 Estabrook RW (1967) Mitochondrial respiratory control and the polarographic measurement of ADP:O ratios.
1547 Methods Enzymol 10:41-7.
1548 Faber C, Zhu ZJ, Castellino S, Wagner DS, Brown RH, Peterson RA, Gates L, Barton J, Bickett M, Hagerty L,
1549 Kimbrough C, Sola M, Bailey D, Jordan H, Elangbam CS (2014) Cardiolipin profiles as a potential
1550 biomarker of mitochondrial health in diet-induced obese mice subjected to exercise, diet-restriction and
1551 ephedrine treatment. J Appl Toxicol 34:1122-9.
1552 Fell D (1997) Understanding the control of metabolism. Portland Press.
1553 Garlid KD, Beavis AD, Ratkje SK (1989) On the nature of ion leaks in energy-transducing membranes. Biochim
1554 Biophys Acta 976:109-20.
1555 Garlid KD, Semrad C, Zinchenko V. Does redox slip contribute significantly to mitochondrial respiration? In:
1556 Schuster S, Rigoulet M, Ouhabi R, Mazat J-P, eds (1993) Modern trends in biothermokinetics. Plenum Press,
1557 New York, London:287-93.
1558 Gerö D, Szabo C (2016) Glucocorticoids suppress mitochondrial oxidant production via upregulation of
1559 uncoupling protein 2 in hyperglycemic endothelial cells. PLoS One 11:e0154813.

1560 Gnaiger E. Efficiency and power strategies under hypoxia. Is low efficiency at high glycolytic ATP production a
1561 paradox? In: Surviving Hypoxia: Mechanisms of Control and Adaptation. Hochachka PW, Lutz PL, Sick T,
1562 Rosenthal M, Van den Thillart G, eds (1993a) CRC Press, Boca Raton, Ann Arbor, London, Tokyo:77-109.
1563 Gnaiger E (1993b) Nonequilibrium thermodynamics of energy transformations. Pure Appl Chem 65:1983-2002.
1564 Gnaiger E (2001) Bioenergetics at low oxygen: dependence of respiration and phosphorylation on oxygen and
1565 adenosine diphosphate supply. Respir Physiol 128:277-97.
1566 Gnaiger E (2009) Capacity of oxidative phosphorylation in human skeletal muscle. New perspectives of
1567 mitochondrial physiology. Int J Biochem Cell Biol 41:1837-45.
1568 Gnaiger E (2014) Mitochondrial pathways and respiratory control. An introduction to OXPHOS analysis. 4th ed.
1569 Mitochondr Physiol Network 19.12. Oroboros MiPNet Publications, Innsbruck:80 pp.
1570 Gnaiger E, Méndez G, Hand SC (2000) High phosphorylation efficiency and depression of uncoupled respiration
1571 in mitochondria under hypoxia. Proc Natl Acad Sci USA 97:11080-5.
1572 Greggio C, Jha P, Kulkarni SS, Lagarrigue S, Broskey NT, Boutant M, Wang X, Conde Alonso S, Ofori E,
1573 Auwerx J, Cantó C, Amati F (2017) Enhanced respiratory chain supercomplex formation in response to
1574 exercise in human skeletal muscle. Cell Metab 25:301-11.
1575 Hinkle PC (2005) P/O ratios of mitochondrial oxidative phosphorylation. Biochim Biophys Acta 1706:1-11.
1576 Hofstadter DR (1979) Gödel, Escher, Bach: An eternal golden braid. A metaphorical fugue on minds and
1577 machines in the spirit of Lewis Carroll. Harvester Press:499 pp.
1578 Illaste A, Laasmaa M, Peterson P, Vendelin M (2012) Analysis of molecular movement reveals latticelike
1579 obstructions to diffusion in heart muscle cells. Biophys J 102:739-48.
1580 Jasienski M, Bazzaz FA (1999) The fallacy of ratios and the testability of models in biology. Oikos 84:321-26.
1581 Jepihhina N, Beraud N, Sepp M, Birkedal R, Vendelin M (2011) Permeabilized rat cardiomyocyte response
1582 demonstrates intracellular origin of diffusion obstacles. Biophys J 101:2112-21.
1583 Klepinin A, Ounpuu L, Guzun R, Chekulayev V, Timohhina N, Tepp K, Shevchuk I, Schlattner U, Kaambre T
1584 (2016) Simple oxygraphic analysis for the presence of adenylate kinase 1 and 2 in normal and tumor cells. J
1585 Bioenerg Biomembr 48:531-48.
1586 Klingenberg M (2017) UCP1 - A sophisticated energy valve. Biochimie 134:19-27.
1587 Koit A, Shevchuk I, Ounpuu L, Klepinin A, Chekulayev V, Timohhina N, Tepp K, Puurand M,Truu L, Heck K,
1588 Valvere V, Guzun R, Kaambre T (2017) Mitochondrial respiration in human colorectal and breast cancer
1589 clinical material is regulated differently. Oxid Med Cell Longev 1372640.
1590 Komlódi T, Tretter L (2017) Methylene blue stimulates substrate-level phosphorylation catalysed by succinyl-
1591 CoA ligase in the citric acid cycle. Neuropharmacology 123:287-98.
1592 Lane N (2005) Power, sex, suicide: mitochondria and the meaning of life. Oxford University Press:354 pp.
1593 Larsen S, Nielsen J, Neigaard Nielsen C, Nielsen LB, Wibrand F, Stride N, Schroder HD, Boushel RC, Helge
1594 JW, Dela F, Hey-Mogensen M (2012) Biomarkers of mitochondrial content in skeletal muscle of healthy
1595 young human subjects. J Physiol 590:3349-60.
1596 Lee C, Zeng J, Drew BG, Sallam T, Martin-Montalvo A, Wan J, Kim SJ, Mehta H, Hevener AL, de Cabo R,
1597 Cohen P (2015) The mitochondrial-derived peptide MOTS-c promotes metabolic homeostasis and reduces
1598 obesity and insulin resistance. Cell Metab 21:443-54.
1599 Lee SR, Kim HK, Song IS, Youm J, Dizon LA, Jeong SH, Ko TH, Heo HJ, Ko KS, Rhee BD, Kim N, Han J
1600 (2013) Glucocorticoids and their receptors: insights into specific roles in mitochondria. Prog Biophys Mol
1601 Biol 112:44-54.
1602 Leek BT, Mudaliar SR, Henry R, Mathieu-Costello O, Richardson RS (2001) Effect of acute exercise on citrate
1603 synthase activity in untrained and trained human skeletal muscle. Am J Physiol Regul Integr Comp Physiol
1604 280:R441-7.
1605 Lemieux H, Blier PU, Gnaiger E (2017) Remodeling pathway control of mitochondrial respiratory capacity by
1606 temperature in mouse heart: electron flow through the Q-junction in permeabilized fibers. Sci Rep 7:2840.
1607 Lenaz G, Tioli G, Falasca AI, Genova ML (2017) Respiratory supercomplexes in mitochondria. In: Mechanisms
1608 of primary energy trasduction in biology. M Wikstrom (ed) Royal Society of Chemistry Publishing, London,
1609 UK:296-337.
1610 Margulis L (1970) Origin of eukaryotic cells. New Haven: Yale University Press.
1611 Meinild Lundby AK, Jacobs RA, Gehrig S, de Leur J, Hauser M, Bonne TC, Flück D, Dandanell S, Kirk N,
1612 Kaech A, Ziegler U, Larsen S, Lundby C (2018) Exercise training increases skeletal muscle mitochondrial
1613 volume density by enlargement of existing mitochondria and not de novo biogenesis. Acta Physiol 222,
1614 e12905.
1615 Menshikova EV, Ritov VB, Fairfull L, Ferrell RE, Kelley DE, Goodpaster BH (2006) Effects of exercise on
1616 mitochondrial content and function in aging human skeletal muscle. J Gerontol A Biol Sci Med Sci 61:534-
1617 40.
1618 Menshikova EV, Ritov VB, Ferrell RE, Azuma K, Goodpaster BH, Kelley DE (2007) Characteristics of skeletal
1619 muscle mitochondrial biogenesis induced by moderate-intensity exercise and weight loss in obesity. J Appl
1620 Physiol (1985) 103:21-7.

1621 Menshikova EV, Ritov VB, Toledo FG, Ferrell RE, Goodpaster BH, Kelley DE (2005) Effects of weight loss
1622 and physical activity on skeletal muscle mitochondrial function in obesity. Am J Physiol Endocrinol Metab
1623 288:E818-25.
1624 Miller GA (1991) The science of words. Scientific American Library New York:276 pp.
1625 Mitchell P (1961) Coupling of phosphorylation to electron and hydrogen transfer by a chemi-osmotic type of
1626 mechanism. Nature 191:144-8.
1627 Mitchell P (2011) Chemiosmotic coupling in oxidative and photosynthetic phosphorylation. Biochim Biophys
1628 Acta Bioenergetics 1807:1507-38.
1629 Mogensen M, Sahlin K, Fernström M, Glintborg D, Vind BF, Beck-Nielsen H, Højlund K (2007) Mitochondrial
1630 respiration is decreased in skeletal muscle of patients with type 2 diabetes. Diabetes 56:1592-9.
1631 Mohr PJ, Phillips WD (2015) Dimensionless units in the SI. Metrologia 52:40-7.
1632 Moreno M, Giacco A, Di Munno C, Goglia F (2017) Direct and rapid effects of 3,5-diiodo-L-thyronine (T2).
1633 Mol Cell Endocrinol 7207:30092-8.
1634 Morrow RM, Picard M, Derbeneva O, Leipzig J, McManus MJ, Gouspillou G, Barbat-Artigas S, Dos Santos C,
1635 Hepple RT, Murdock DG, Wallace DC (2017) Mitochondrial energy deficiency leads to hyperproliferation of
1636 skeletal muscle mitochondria and enhanced insulin sensitivity. Proc Natl Acad Sci U S A 114:2705-10.
1637 Murley A, Nunnari J (2016) The emerging network of mitochondria-organelle contacts. Mol Cell 61:648-53.
1638 National Academies of Sciences, Engineering, and Medicine (2018) International coordination for science data
1639 infrastructure: Proceedings of a workshop—in brief. Washington, DC: The National Academies Press. doi:
1640 https://doi.org/10.17226/25015.
1641 Palmfeldt J, Bross P (2017) Proteomics of human mitochondria. Mitochondrion 33:2-14.
1642 Paradies G, Paradies V, De Benedictis V, Ruggiero FM, Petrosillo G (2014) Functional role of cardiolipin in
1643 mitochondrial bioenergetics. Biochim Biophys Acta 1837:408-17.
1644 Pesta D, Gnaiger E (2012) High-Resolution Respirometry. OXPHOS protocols for human cells and
1645 permeabilized fibres from small biopsies of human muscle. Methods Mol Biol 810:25-58.
1646 Pesta D, Hoppel F, Macek C, Messner H, Faulhaber M, Kobel C, Parson W, Burtscher M, Schocke M, Gnaiger
1647 E (2011) Similar qualitative and quantitative changes of mitochondrial respiration following strength and
1648 endurance training in normoxia and hypoxia in sedentary humans. Am J Physiol Regul Integr Comp Physiol
1649 301:R1078–87.
1650 Price TM, Dai Q (2015) The role of a mitochondrial progesterone receptor (PR-M) in progesterone action.
1651 Semin Reprod Med 33:185-94.
1652 Puchowicz MA, Varnes ME, Cohen BH, Friedman NR, Kerr DS, Hoppel CL (2004) Oxidative phosphorylation
1653 analysis: assessing the integrated functional activity of human skeletal muscle mitochondria – case studies.
1654 Mitochondrion 4:377-85. Puntschart A, Claassen H, Jostarndt K, Hoppeler H, Billeter R (1995) mRNAs of
1655 enzymes involved in energy metabolism and mtDNA are increased in endurance-trained athletes. Am J
1656 Physiol 269:C619-25.
1657 Quiros PM, Mottis A, Auwerx J (2016) Mitonuclear communication in homeostasis and stress. Nat Rev Mol
1658 Cell Biol 17:213-26.
1659 Rackham O, Mercer TR, Filipovska A (2012) The human mitochondrial transcriptome and the RNA-binding
1660 proteins that regulate its expression. WIREs RNA 3:675–95.
1661 Reichmann H, Hoppeler H, Mathieu-Costello O, von Bergen F, Pette D (1985) Biochemical and ultrastructural
1662 changes of skeletal muscle mitochondria after chronic electrical stimulation in rabbits. Pflugers Arch 404:1-
1663 9.
1664 Renner K, Amberger A, Konwalinka G, Gnaiger E (2003) Changes of mitochondrial respiration, mitochondrial
1665 content and cell size after induction of apoptosis in leukemia cells. Biochim Biophys Acta 1642:115-23.
1666 Rich P (2003) Chemiosmotic coupling: The cost of living. Nature 421:583.
1667 Rostovtseva TK, Sheldon KL, Hassanzadeh E, Monge C, Saks V, Bezrukov SM, Sackett DL (2008) Tubulin
1668 binding blocks mitochondrial voltage-dependent anion channel and regulates respiration. Proc Natl Acad Sci
1669 USA 105:18746-51.
1670 Rustin P, Parfait B, Chretien D, Bourgeron T, Djouadi F, Bastin J, Rötig A, Munnich A (1996) Fluxes of
1671 nicotinamide adenine dinucleotides through mitochondrial membranes in human cultured cells. J Biol Chem
1672 271:14785-90.
1673 Saks VA, Veksler VI, Kuznetsov AV, Kay L, Sikk P, Tiivel T, Tranqui L, Olivares J, Winkler K, Wiedemann F,
1674 Kunz WS (1998) Permeabilised cell and skinned fiber techniques in studies of mitochondrial function in
1675 vivo. Mol Cell Biochem 184:81-100.
1676 Salabei JK, Gibb AA, Hill BG (2014) Comprehensive measurement of respiratory activity in permeabilized cells
1677 using extracellular flux analysis. Nat Protoc 9:421-38.
1678 Sazanov LA (2015) A giant molecular proton pump: structure and mechanism of respiratory complex I. Nat Rev
1679 Mol Cell Biol 16:375-88.
1680 Schneider TD (2006) Claude Shannon: biologist. The founder of information theory used biology to formulate
1681 the channel capacity. IEEE Eng Med Biol Mag 25:30-3.

1682 Schönfeld P, Dymkowska D, Wojtczak L (2009) Acyl-CoA-induced generation of reactive oxygen species in
1683 mitochondrial preparations is due to the presence of peroxisomes. Free Radic Biol Med 47:503-9.
1684 Schultz J, Wiesner RJ (2000) Proliferation of mitochondria in chronically stimulated rabbit skeletal muscle--
1685 transcription of mitochondrial genes and copy number of mitochondrial DNA. J Bioenerg Biomembr 32:627-
1686 34.
1687 Speijer D (2016) Being right on Q: shaping eukaryotic evolution. Biochem J 473:4103-27.
1688 Sugiura A, Mattie S, Prudent J, McBride HM (2017) Newly born peroxisomes are a hybrid of mitochondrial and
1689 ER-derived pre-peroxisomes. Nature 542:251-4.
1690 Simson P, Jepihhina N, Laasmaa M, Peterson P, Birkedal R, Vendelin M (2016) Restricted ADP movement in
1691 cardiomyocytes: Cytosolic diffusion obstacles are complemented with a small number of open mitochondrial
1692 voltage-dependent anion channels. J Mol Cell Cardiol 97:197-203.
1693 Stucki JW, Ineichen EA (1974) Energy dissipation by calcium recycling and the efficiency of calcium transport
1694 in rat-liver mitochondria. Eur J Biochem 48:365-75.
1695 Tonkonogi M, Harris B, Sahlin K (1997) Increased activity of citrate synthase in human skeletal muscle after a
1696 single bout of prolonged exercise. Acta Physiol Scand 161:435-6.
1697 Torralba D, Baixauli F, Sánchez-Madrid F (2016) Mitochondria know no boundaries: mechanisms and functions
1698 of intercellular mitochondrial transfer. Front Cell Dev Biol 4:107. eCollection 2016.
1699 Vamecq J, Schepers L, Parmentier G, Mannaerts GP (1987) Inhibition of peroxisomal fatty acyl-CoA oxidase by
1700 antimycin A. Biochem J 248:603-7.
1701 Waczulikova I, Habodaszova D, Cagalinec M, Ferko M, Ulicna O, Mateasik A, Sikurova L, Ziegelhöffer A
1702 (2007) Mitochondrial membrane fluidity, potential, and calcium transients in the myocardium from acute
1703 diabetic rats. Can J Physiol Pharmacol 85:372-81.
1704 Wagner BA, Venkataraman S, Buettner GR (2011) The rate of oxygen utilization by cells. Free Radic Biol Med
1705 51:700-712.
1706 Wang H, Hiatt WR, Barstow TJ, Brass EP (1999) Relationships between muscle mitochondrial DNA content,
1707 mitochondrial enzyme activity and oxidative capacity in man: alterations with disease. Eur J Appl Physiol
1708 Occup Physiol 80:22-7.
1709 Watt IN, Montgomery MG, Runswick MJ, Leslie AG, Walker JE (2010) Bioenergetic cost of making an
1710 adenosine triphosphate molecule in animal mitochondria. Proc Natl Acad Sci U S A 107:16823-7.
1711 Weibel ER, Hoppeler H (2005) Exercise-induced maximal metabolic rate scales with muscle aerobic capacity. J
1712 Exp Biol 208:1635–44.
1713 White DJ, Wolff JN, Pierson M, Gemmell NJ (2008) Revealing the hidden complexities of mtDNA inheritance.
1714 Mol Ecol 17:4925–42.
1715 Wikström M, Hummer G (2012) Stoichiometry of proton translocation by respiratory complex I and its
1716 mechanistic implications. Proc Natl Acad Sci U S A 109:4431-6.
1717 Williams EG, Wu Y, Jha P, Dubuis S, Blattmann P, Argmann CA, Houten SM, Amariuta T, Wolski W,
1718 Zamboni N, Aebersold R, Auwerx J (2016) Systems proteomics of liver mitochondria function. Science 352
1719 (6291):aad0189
1720 Willis WT, Jackman MR, Messer JI, Kuzmiak-Glancy S, Glancy B (2016) A simple hydraulic analog model of
1721 oxidative phosphorylation. Med Sci Sports Exerc 48:990-1000.
1722